

CHAPTER 3

LANDFORMS INDICATIVE OF CREEP OF DEBRIS AND ICE

Among the large number of landforms related to the creep of ice and debris in periglacial environments on Earth, the most well-known landforms comprise rock glaciers and landforms related to gelifluction processes. While rock glaciers usually form relatively confined but well-distinct landforms, the latter contribute to a large extent to the general slope development in periglacial environments and are less distinct in their appearance. The author focuses here on rock glaciers and related landforms because of their size which allows comparison work with landforms on Mars and because of their direct connection to so-called Martian lobate debris aprons which are discussed in subsequent sections. Slope-forming processes in contrast to this, cover a much wider field that is characterized by an abundance of landforms that cannot be attributed to a distinct climatic environment unambiguously because of their transitional nature (e.g., *Selby, 1982*). Also, terrestrial slope-forming processes are not necessarily comparable to the Martian environment because of the nature of controlling factors, such as vegetation and precipitation. The subsequent discussion of rock glaciers and related landforms on Earth will not only summarize some of the major scientific aspects but will also try to establish a connection to the Martian environment whenever possible.

3.1. Terrestrial Rock Glaciers

3.1.1. Definitions and Classifications

The definition of the term *rock glacier* has undergone several modifications and is even after more than one century of research and investigations characterized by misinterpretations and forms the basis for many debates in the community (*Barsch, 1996*). Although the wording *rock glacier* implies a connection to "true" glaciers, rock glaciers are different from glaciers not only compositionally but also in terms of mechanics, deformation and with respect to associated climatic implications. Except for their size and often lobate- (width > length, figure 3.1) to tongue-shaped (width < length, figure 3.2) morphology, rock glaciers have not much in common with glaciers. As *Haeberli (1985)*, p. 7 emphasizes, rock glaciers are "*neither a question of rocks nor of glaciers, but of creep phenomena in Alpine permafrost*" and are characterized by "*perenni-*

ally frozen debris masses which creep down mountain slopes [...] similar to the behaviour of lava streams".

Some definitions focus on morphology by saying that a rock glacier is "*an accumulation of angular rock debris, usually with a distinct ridge/furrow pattern and steep front and side slopes, whose length is generally greater than its width: existing on a valley floor*" (*Martin and Whalley, 1987; Hamilton and Whalley, 1995*). This definition also covers ice-cored moraines, debris covered glaciers, permafrost creep features, glacial ice-cored rock glaciers and certain types of landslides (*Hamilton and Whalley, 1995*) but it does not necessarily include rock-glacier landforms whose width is much larger than the length as typical for protalus lobes that are usually included in the feature class of rock glaciers and are often called "valley-wall rock glaciers" (*Whalley, 1992*). Other examples are

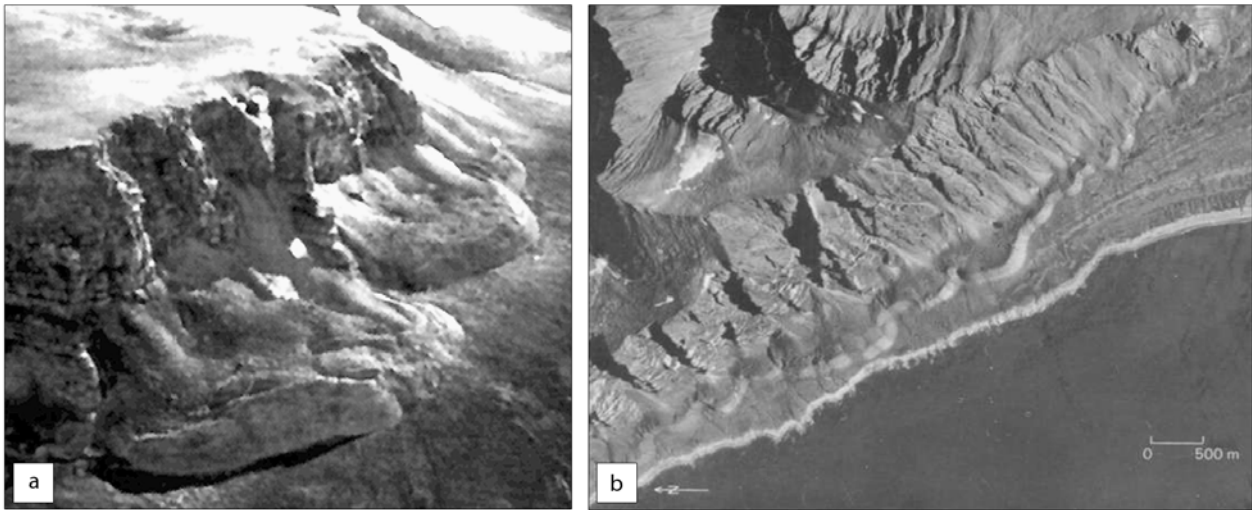


Figure 3.1.: Terrestrial protalus landforms: [a] lobate rock glacier (protalus rock glacier) at the footslope of an escarpment on Stuphallet, Bröggerhalvöja, western Svalbard (Barsch, 1996, p. 10); [b] western shore of Prins Karls Forland, aerial photograph Norsk Polarinstitut, Oslo, Norway (André, 1994, p. 240).

moraines that can produce rock-glacier landforms but are not connected to talus deposits and also form landforms where the width extends the length (Luckman and Crocket (1978) and Luckman and Osborn (1979) as cited in Hamilton and Whalley (1995)). Most confusion is caused by the discussion on the synthesis of lobate rock glaciers and protalus landforms that are morphologically different to a certain degree and have undergone a quite different formation. Nonetheless, both landforms are considered as rock glaciers and are discussed as such in literature.

A large number of definitions exist that have been considered being too restrictive. These definitions are often based upon different foci that cover mostly just one aspect extensively while other aspects are omitted. Some of the important aspects are summarized by Hamilton and Whalley (1995) and cover (a) overall morphology, describing rock glaciers as either lobate or tongue-shaped to spatulate (Wahrhaftig and Cox, 1959), (b) process of formation, covering ice-cored and ice-cemented rock glaciers (White, 1971; Potter, 1972), (c) topographic position as defined by valley-wall and valley-floor rock glaciers (Outcalt and Benedict, 1965), and (d) state of dynamics discussing whether these landforms are active, inactive or fossil (Wahrhaftig and Cox, 1959; Haeberli, 1985;

Barsch, 1996). Even more confusing is that identical landforms have been described by various authors using different approaches in different ways, e.g., the so-called lobate and tongue-shaped landforms of Wahrhaftig and Cox (1959) have been discussed as valley-side and valley-floor rock glaciers by Outcalt and Benedict (1965) (table 3.1).

The official definition given by the International Permafrost Association (IPA) states that a rock glacier is "a mass of rock fragments and finer material, on a slope, that contains either interstitial ice or an ice core and shows evidence of past or present movement" (van Everdingen, 2005, p. 63). When comparing this definition to the points summarized by Hamilton and Whalley (1995), it becomes obvious that only few aspects are covered and that issues such as environmental and formation conditions are not included in this definition. In the explanations given by van Everdingen (2005) for the IPA definition, however, some additional words are said regarding the availability of sufficient moisture which must be available in order to form interstitial ice and to allow movement of the rocky debris. Furthermore, surficial characteristics such as transverse ridges and furrows as discussed by Martin and Whalley (1987) are also mentioned in the IPA explanations (van Everdingen,

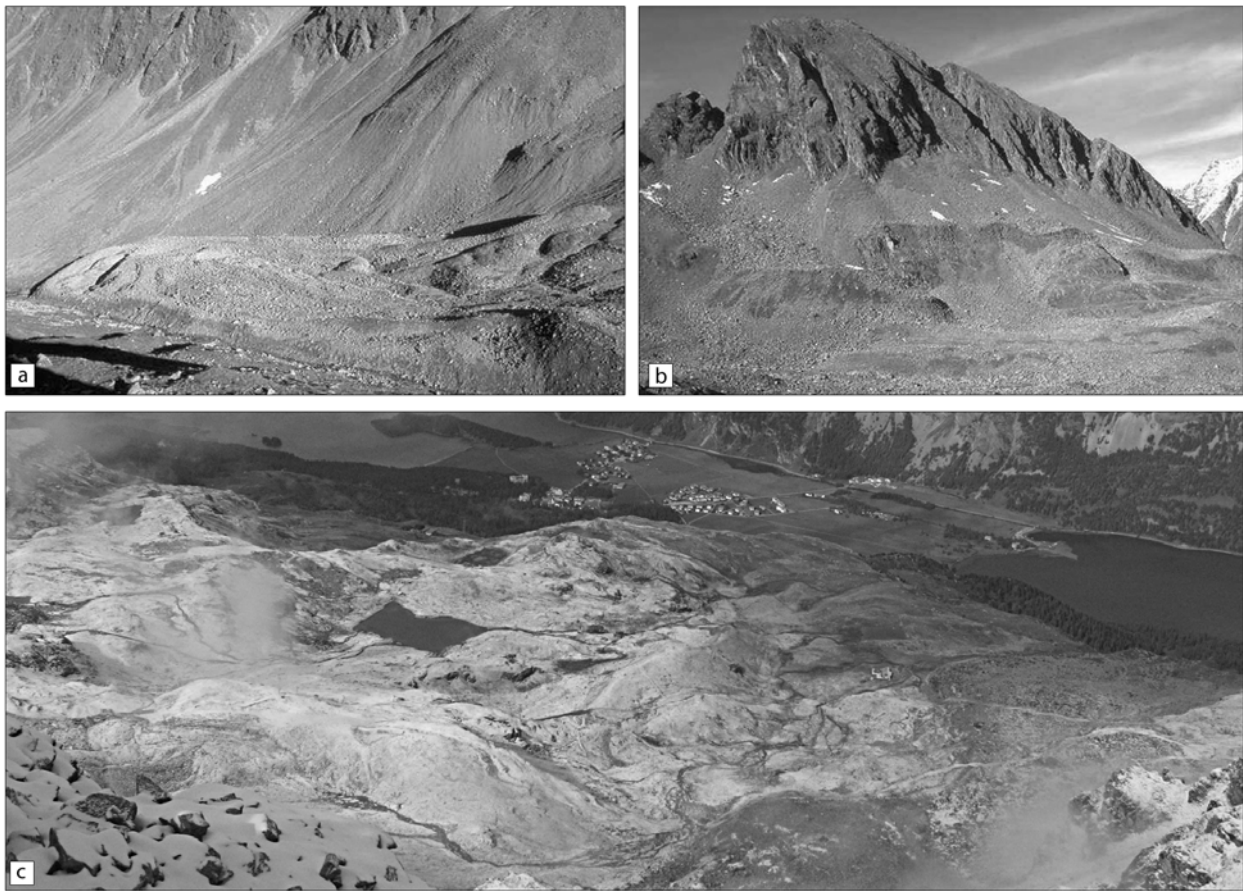


Figure 3.2.: Terrestrial rock glacier landforms: [a] tongue-shaped fossil rock glacier in Kaiserberg Valley, Ötztal Alps, valley-floor type, photograph: Rock Glacier Working Group, University of Innsbruck; [b] fossil talus rock glacier, Rosskar, Stubai Alps, valley-wall type, photograph: Rock Glacier Working Group, University of Innsbruck; [c] Murtel rock glacier, Piz Corvatsch, photograph: S. van Gasselt, 2006.

gen, 2005). (Barsch, 1988, 1992) defines a rock glacier on the basis of its connection to permafrost by saying that so-called permafrost rock glaciers are the only "true" rock glaciers whereas other morphologically and topographically similar looking landforms are simply something else. This statement does implicitly say that formation of rock glaciers must be connected to a specific genetic model of formation which then allows unambiguously to attribute a certain landform as defined by its morphology to a specific process. As put forward by Hamilton and Whalley (1995), this view contradicts statements which say that similar-looking landforms can be formed by different processes as initially emphasized by, e.g., Vick (1987).

Further on, Barsch (1988, 1996) defines active rock glaciers as "lobate or tongue-shaped bodies of perennially frozen unconsolidated material supersaturated with interstitial ice and ice lenses that move downslope or downvalley by creep as a consequence of the deformation of ice contained in them and which are, thus, features of cohesive flow". Barsch (1996) also refers to the definition of Haeblerli (1985) who defined active rock glaciers as "a visible expression of steady-state creep of ice-supersaturated mountain permafrost bodies in unconsolidated materials. They display the whole spectrum of forms created by cohesive flow" (Haeblerli, 1985). Barsch (1996) emphasizes that the three most important aspects are covered by this definition: (1) process, i.e., the creep of moun-

Table 3.1: Rock-glacier nomenclature and types as defined by various authors, from *Hamilton and Whalley (1995)* after *Whalley (1992)*, see also figure 3.3.

author	wide landforms	elongated landforms
<i>Barsch (1988)</i>	talus rock glacier	debris rock glacier
<i>Outcalt and Benedict (1965)</i>	valley-side rock glacier	valley-floor rock glacier
<i>Wahrhaftig and Cox (1959)</i>	lobate rock glacier	tongue-shaped rock glacier
<i>Lindner and Marks (1985)</i>	protalus rock glacier	moraine rock glacier
<i>Whalley (1992)</i>	protalus lobe	rock glacier

tain permafrost supersaturated with ice, (2) material, i.e., unconsolidated frozen rock fragments derived from talus slopes, moraines and other sources, and (3) form, i.e., generally tongue- or lobate shaped.

Beside a proper definition, the taxonomic classification of rock glaciers is even more confusing and has been extensively discussed by e.g., *Corte (1987)*. This topic does not require detailed repetitive work although some of the most relevant issues will be summarized for reference. Genetically, *Corte (1987)* distinguishes four rock glacier groups:

(1) *glaciogenic rock glaciers* are rock glaciers that are related to glaciers and consist of perennially frozen debris bodies, i.e., permafrost, that are covered by debris that is essentially unfrozen and forms an active layer; these landforms have been described by other workers in the past using a variety of terms, including e.g., debris-covered glaciers (e.g., *Lliboutry, 1955; Corte, 1976*), ice-cored moraines (*Östrem, 1966*), or ablation complexes (*Johnson, 1978*); see also *Corte (1987)*. These terminological approaches do by no means say that debris-covered glaciers and glaciogenic rock glaciers derived from moraines are basically the same type of landforms or have undergone identical processes, their common nature is that they are connected to glacial ice.

(2) The second group contains so-called *avalanche-debris rock glaciers* which are composed of frozen debris with layers of firn-ice and debris derived from avalanches and cryogenic action and which show well-developed transverse and longitudinal ridges. Descriptions such as valley-wall type, talus- and slope-type rock glaciers (*Barsch, 1969, 1983*), lobate rock glaciers (*White, 1976*), and rockfall talus rock

streams (*Tyurin (1983)* as cited in *Corte (1987)*) belong to this group.

(3) Rock glaciers below boulder fields and gelifluction streams are termed *gelifluction rock glaciers* and are different from avalanche-debris rock glaciers as they are rather small and are only located at the footslope below wall-rock. Debris material is incorporated by rock fall and gelifluction processes mainly and surface characteristics are limited to transverse ridges.

(4) According to *Corte (1987)*, the last group comprises all other genetic types that can not be categorized properly in one of the three other groups. *Barsch (1978)*, in contrast, has a more pragmatic approach saying that there are basically two types of rock glaciers: one being derived from talus deposits (*talus rock glacier*, figure 3.1) and one group that is derived from moraine deposits (*debris rock glacier*). Further classification could be made with respect to either the current state or the morphological appearance, i.e., relief, form, shape, size, geomorphologic location (*Barsch, 1978*). The present state of rock glaciers is also covered in several definitions and include (a) *active rock glaciers* being rock glaciers that move at present with velocities of $0.1-1 \text{ ma}^{-1}$, (b) *inactive rock glaciers* that are not moving anymore, and (c) *fossil* or *relict rock glacier* being rock glaciers in which all ice is gone and which are characterized by collapse structures and a generally degraded appearance. Inactive rock glaciers do not move at present because of melting of included ice, i.e., they are climatically inactive (*Barsch, 1973*), or because of other factors such as detachment from the source area or a decrease of stress. If the rock glacier is situated in continuous permafrost (*Ellis and Calkin, 1984; Sollid*

and Sörbel, 1992) and melting of ice is not responsible for its inactivity, it is called *dynamic inactive* (Barsch, 1996). For more details and alternative categories the reader is referred to Barsch (1996), p. 9ff (figure 3.3). It becomes obvious from the two selected classification schemes presented above that transitional morphologies can and do exist and that any classification is an attempt to categorize all the different types of features that have been mentioned in research history. In addition, these naming attempts illustrate the difficulties in finding a naming scheme that is based upon the genetic relationships and that also comprises some of the relevant morphological aspects. No definition will probably satisfy completely as too many landforms exist that are similar with respect to morphology or process but that are different in other aspects. Rock glaciers are one of the more complicated landforms in terrestrial periglacial environments. This fact is caused significantly by their environmental response manifested in their morphology and the way ice is incorporated and how it affects movement of a rock glacier.

All different morphological types and origins of rock glaciers are affected by the environmental conditions and changes of these conditions. Corte (1987) summarizes these controlling factors which are grouped into *static factors* as expressed by the erodability of wall-rock material controlled by e.g., joints and susceptibility to fracturing, and *climato-dynamic factors* that are expressed by mean temperature regimes, amounts of precipitation and contribution of moisture. Other controlling factors comprise *latitudinal-altitudinal factors* that account for changes in temperature and finally the so-called *inherited paleoclimate*, that consists of all consequential aspects connected to formerly glaciated terrain with respect to local topographies and supply of material but it also comprises climatic change that causes variations in e.g., freeze-thaw cycles.

Although a rich amount of literature on terrestrial rock glaciers exist, investigations are often limited due to their generally limited economical importance. There is some potential for geologic hazards to populated places although rock-glacier movement is

rather slow but catastrophic release of water can occur putting rock glaciers in the same hazard category as landslides and active faults (Giardino and Vick, 1987). Most of the economically relevant research focuses on the ability of rock glaciers to store large amount of water even in arid regions (see preface by C. Wahrhaftig in Giardino et al. (1987), p. xii). From the scientific point of view, however, rock glaciers are important indicators not only for the present but also for past climates in certain areas as their existence is connected to the distribution of permafrost.

By distinguishing active, relict and fossil rock glaciers, implications and understanding of climatic fluctuations can be achieved and the timing for major climate changes can be estimated. Rock glacier origins and systematics are extensively discussed in a relatively recent monograph by Barsch (1996) and a collection of contributions edited by Giardino et al. (1987). New work on rock glaciers, their morphology, climate implications and deformation mechanics is published almost weekly and some of the most fundamental issues will be discussed in the following sections.

For simplicity reasons and comparability to Martian landforms, in this study rock glaciers are considered simply as masses of angular debris and finer-grained materials that have been transported downslope by creep processes and that were derived from landsliding or talus produced by rock fall and which undergoes viscous deformation. Ice is considered to be distributed interstitially or as ice lenses (lenticular) within the body of the rock glacier. The source of ice and the environmental border conditions, however, need additional discussion because they are not only of terminological importance but they need to be understood in order to achieve a proper knowledge of the morphology and characteristics that similar landforms in different environments, such as Mars, can have.

3.1.2. Rock-Glacier Origin and Composition

The earliest work on rock glacier landforms was published in literature on landforms in Greenland (Steen-

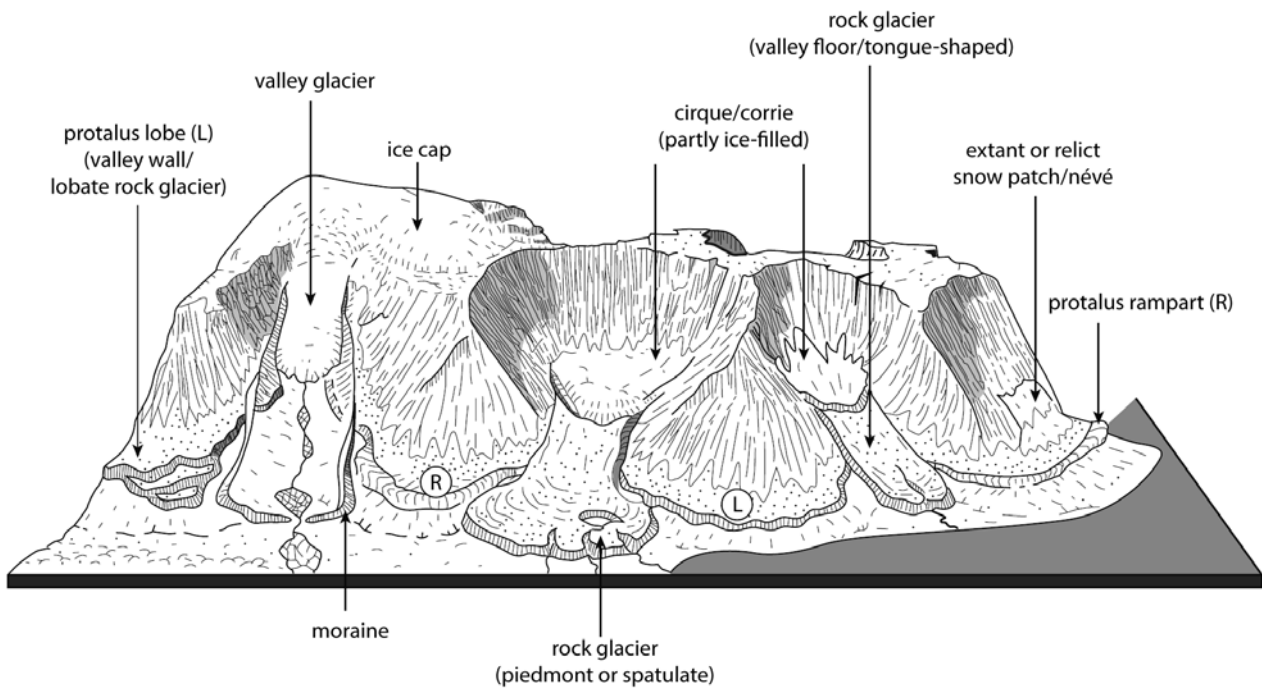


Figure 3.3.: Debris-ice systems in mountainous areas including terminology and alternative terms in parentheses. After *Martin and Whalley (1987)*, *Humlum (1988)*, and *Hamilton and Whalley (1995)* in *Whalley and Azizi (2003)*, modified.

strup (1883) as cited in *Barsch (1996)* and *Humlum (1982)*; *Spencer (1900)* as cited in *Wahrhaftig and Cox (1959)*).

The first mentioning of the term "rock glacier", however, is attributed to *Capps (1910)* in his work on such landforms in the Alaska Wrangell Mountains. Since then, the term "rock glacier" has undergone several modifications and a variety of theories have been put forward to explain the nature of these landforms. While first explanations discussed these features as "unusual type of moraine" (*Cross and Howe, 1905*), later work discussed these features as debris from high-energetic landslides (*Howe, 1909*). A completely different mechanism was considered by *Capps (1910)* who suggested that water from melting ice or precipitation (or springs according to *Tyrell (1910)*) fills up pore spaces in debris collected at the terminus of glaciers up to level where melting equals freezing resulting in movement of ice through freeze-melt cycles (*Capps (1910)* after *Spencer (1900)*). Later theories suggest that rock glaciers were essentially ter-

minal glacial moraines. Pore space would be filled by frozen mud and clay that freezes and thaw and cause subsequently movement of the debris (*Chaix, 1923*). The glacial aspect for rock glacier origins and formation was later put forward by *Kesseli (1941)* discussing rock glaciers as relict ice cores, and *Richmond (1952)* who believed that rock glaciers are simply relics of earlier glacial advances and therefore are characterized by the same configuration of ice as the main glacier they are derived from. Movement would then be confined to an upper unfrozen layer similar to surficial creep and solifluction (*Richmond, 1952*).

Basis for scientific investigations today and one of the most extensive field works on rock glaciers was performed by *Wahrhaftig and Cox (1959)* extending the work by *Wahrhaftig (1954)* by discussing a variety of aspects of rock glaciers in the Healy area of the Alaska Range. They made a comprehensive study of landforms discussing not only deformation mechanisms but also discussing the state of rock glaciers and their climate response and provided a detailed descriptions

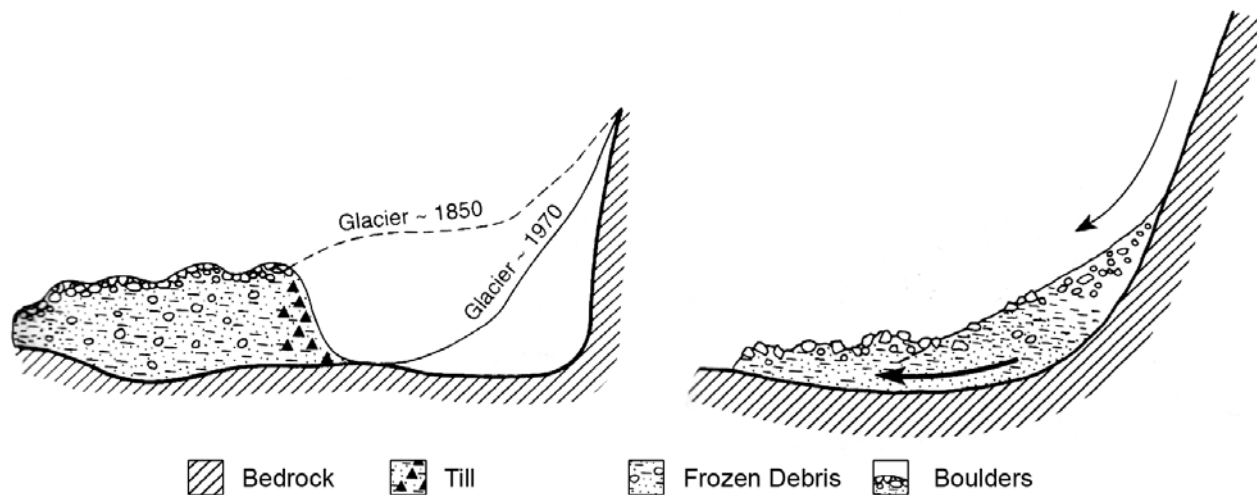


Figure 3.4.: Rock glacier models according to *Barsch* (1988). Debris "rockglacier" below glacier that is derived from moraine material (left) and talus "rockglacier" derived from weathered rock material incorporated into talus deposits.

on the shape and microrelief of rock glaciers.

In the upcoming years scientific investigations were split into two fields, one group considered rock glaciers simply as debris-covered glaciers (*Potter, 1972; Johnson, 1974*) while other workers in that field considered these as periglacial landforms (*Barsch, 1978, 1988; Haerberli, 1985*). According to *Wahrhaftig and Cox (1959)*, rock glaciers are simply one type of glaciers with all hypothetical gradations between rock glaciers and glaciers. But they state also that the circumstances under which ice is formed and preserved in rock glaciers is different from glacial systems and the climatic environment does not necessarily allow intermediate forms.

Even today this dispute has not been completely settled yet as it would require in-depth field experiments to obtain information on the internal structure of these features. According to *Barsch (1988)*, none of the field work conducted thus far had proven that rock glaciers should be considered as debris-covered glaciers. Further on, he suggests that two basic types of periglacial rock glaciers need to be distinguished: those landforms occurring below talus deposits (*talus rockglaciers*) and those below glaciers (*debris rockglacier*¹, figure 3.4). In both cases, a significant de-

bris supply is required which is derived from rock-weathered material on a talus or from moraines below glaciers. Ice is derived from melting of snow and infiltration of meltwater into pore spaces so that a matrix of ice and debris is formed which is able to deform gradually during downward movement. *Wahrhaftig and Cox (1959)* summarize the essential conditions for formation of rock glaciers which are still considered to be valid even today and that consist of (a) an abundant supply of coarse debris and (b) a climate conducive to the accumulation of interstitial ice.

Prerequisites for rock-glacier formation are high and steep cliffs commonly found at valley sides or glacial cirques as well as mean temperatures below 0°C in order to maintain ice within the pore space. An important climatic aspect is that the climate needs to be similar to glacial environments with an abundance of moisture available but without the accumulation of snow required for glacial environments; this translates to a *near-glacial permafrost climate* (*Wahrhaftig and Cox, 1959*). The other issue necessary for rock glacier formation are large blocks of debris that can collect at a footslope and provide the necessary load for the underlying ice to deform under the overburden. It has been shown early that rock glaciers

¹Note, *Barsch (1992)* introduced the term *rockglacier* (instead of *rock glacier*) in order to separate this landform from common glaciers

are generally derived from frost-shattered debris and rock-fall material below cliffs where large talus deposits are formed. Their composition therefore reflects the local lithology of surrounding massifs and valley walls.

Rock glaciers normally show an upper layer of rubble and blocky debris and a much finer-grained layer of debris underneath (e.g., *Domaradzki, 1951; Wahrhaftig and Cox, 1959*). Ice was found to have different appearances within a rock glacier body, ranging from interstitial ice cementing the debris from the head to terminus (*Capps, 1910; Wahrhaftig and Cox, 1959*) to massive ice bodies of several meters of thickness (e.g., *Domaradzki, 1951*). Completely ice-free areas are also reported from shallow excavations at the rock glacier's terminus (*Brown (1925)* as cited in *Wahrhaftig and Cox (1959)*). Water can be derived from precipitation, snow drifts or even from permafrost springs forming so-called icings (*Muller, 1947*). These icing, or *chrystocrenes* according to *Tyrell (1910)*, can occur within a debris body and provide the required water and ice to fill the pore spaces in the debris. *Johnson (1978)* summarized formation conditions of different types of rock glaciers: Glacier-debris rock glaciers are considered to have a simple two layer structure composed of a glacial ice core with a thin (up to 3 m) cover of till. These types occur generally at the terminus of cirque glaciers and extend down-valley. Supply of till is controlled by the glaciologic and geologic configuration at the rock glacier location where most of the debris material is supplied at the cirque lips leaving the cirque glacier basically free of debris (*Johnson, 1978*). As soon as the glacier retreats, advance of the rock glacier also stops. Ice-cored lateral moraines often merge with the rock glacier and are reworked into the rock glacier flow. Morphologically, these rock glaciers are characterized by numerous overlapping lobes with slope angles of up to 45°. Individual flow lobes can be deformed by flow ridges and flow of individual lobes over pre-existing ones. This configurations often causes formation of characteristic depression that can subsequently be filled with water.

It is noteworthy that thermokarstic structures nor-

mally do not occur on glacier-debris rock glaciers; the limited occurrence of such features is connected to the thermal activity of meltwater only. Flow occurs through the deformation of the glacier ice and is usually not connected to the deformation of the covering till. *Johnson (1978)* summarizes that flow can occur through the advance of the glacier itself or through deformation of the buried ice after glacier retreat.

The majority of rock glaciers are of a non-glacial origin and are formed through a rich amount of different processes controlled by environmental conditions. The possible different triggers for rock glacier formation of non glacial origin are difficult to combine in a coherent view and need to be stressed separately. Detailed discussions on this topic can be found in *Johnson (1987)*. In general, wall rock must be destabilized to facilitate rock glacier formation and aid subsequent flow. Reasons for instabilities can be caused by glacial unloading, hydrostatic pressure in bedrock or in the unconsolidated overburden, undercutting of wall rock by, e.g., glacial meltwater, snow- and rock avalanching (*Vick, 1987*), melting of ice, and by so-called external causes, such as earthquakes. Many of these processes aid rock-glacier movement and generally cause increase of debris input that leads to oversteepening and subsequent adjustments, i.e., movement, at the terminus of the rock glacier (*Johnson, 1987*).

3.1.3. Global Distribution of Rock Glaciers

In principle, rock glacier landforms can be easily detected in remote sensing data due to their size and characteristic surface texture. The knowledge about the characteristics of rock glaciers has been obtained in the field, especially by geophysical methods, velocity measurements and drilling, or – to a minor degree – by photogrammetrical investigations on the basis of remote sensing data. Rock glaciers are connected to the alpine or high-latitude mountainous periglacial environments and are therefore limited to large mountain systems in Europe and America where they have been studied in great detail 3.5. As *Barsch (1996)* points out, a world-wide systematic summary of their

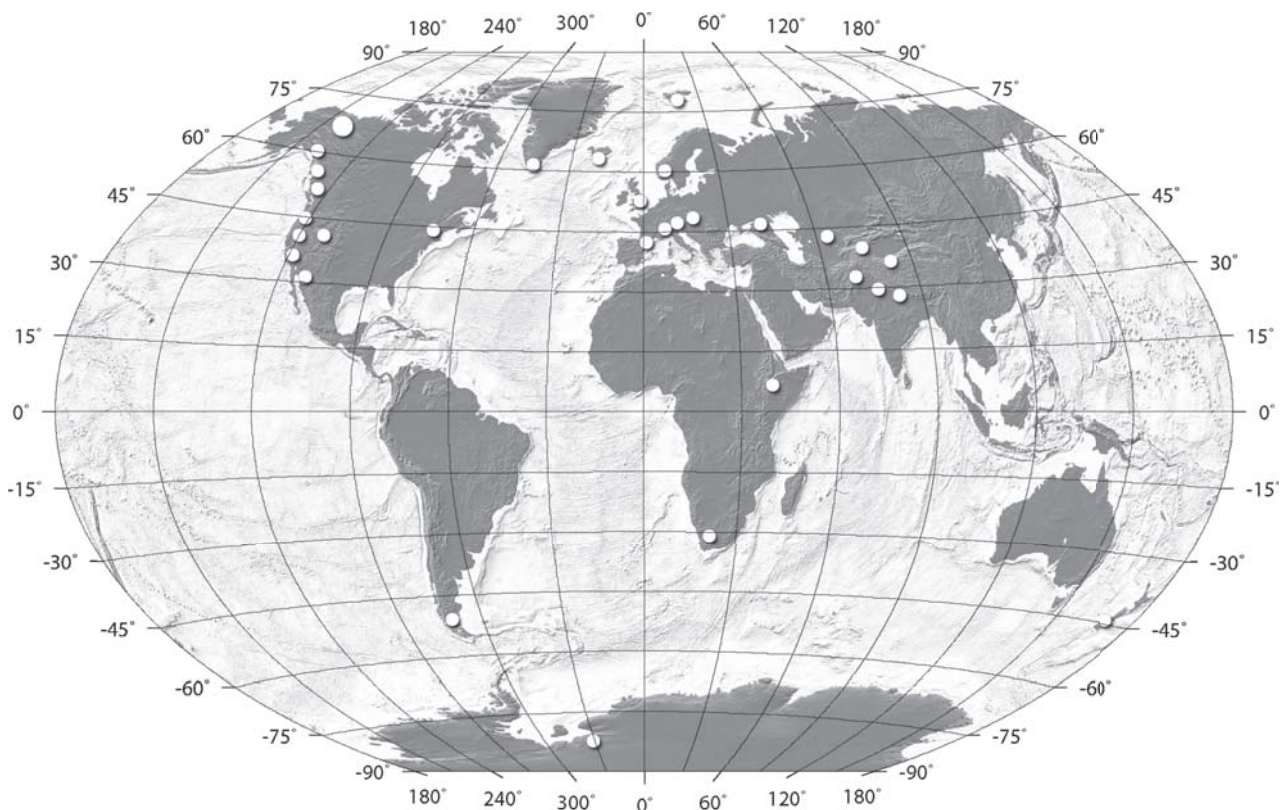


Figure 3.5.: Locations of world-wide study areas of main terrestrial rock glacier research (compilation from references in *Barsch (1996)*).

distribution is still missing; for North America and Europe such a summary has been provided by *Höllermann (1983)*. Rock glaciers have been reported from latitudes covering the Arctic areas of Canada and Greenland to Antarctica and they become relatively rare within the 25° latitude belt except for some high-mountain systems. Climatically, their occurrences are connected to continental dry regions, and they are much less frequent in mediterranean or even humid areas where conditions are more favourable for glacier formation. Except for the climatic control, topography plays an important role as rock glaciers can only develop within valleys or below slopes where the production-rate of talus material is high.

3.1.4. Rock Glaciers Properties

3.1.4.1. Movement of Rock Glaciers

The variety of possible mechanisms causing rock-glacier formation can lead to a variety of transport

mechanisms as summarized by *Johnson (1987)*.

[1] *Creep* is the expression of deformation of ice and debris under applied stresses and forms the primary mechanisms. It will be discussed in detail below.

[2] Movement of masses of cohesionless grains without ice or water form *granular flows* and occurs frequently during slope failures. This process often occurs in connection with landslides and avalanche processes and is characterized by a rapid dissipation of momentum that produces a complex pattern of surface ridges and can also show lateral levees and formation of chutes (*Howe, 1909; Chaix, 1919, 1943; Vick, 1981*).

[3] *Slide mechanisms* are related to the movement of coherent and non-cohesive masses along an inclined plane. Although sliding affects the overall debris mass, the non-cohesive character of grains usually favors formation of a simple lobate form which occurs usually along valley walls rather than on valley floors. Later modification of the landform is caused

by subsequent rock fall or a residual amount of deformation (Johnson, 1987; Giardino, 1979; Giardino and Vitek, 1985).

[4] *Slab mechanisms* involves progressive collapse of the slope which moves away from the base (Johnson, 1987). Successive formation of slabs is considered to cause surface ridges similar to flow ridges and formation of multiple lobes overlapping each other. For more details on this mechanism the reader is referred to e.g., Maxwell (1979) (as cited in Giardino and Vick (1987)) where such models have been described.

[5] More exotic mechanisms comprise processes such as *hydrostatic flow* which occurs if hydrostatic pressure builds up. It is considered to contribute to a minor degree to rock glacier movement as (a) rock fragments lock each other and (b) hydrostatic pressure is released rapidly and limits further advance of the rock glacier. Other less important processes involve *air-cushion mechanisms* that are used to explain long run-out features. According to Johnson (1987) this process' efficiency has not been demonstrated yet and it only applies to very long run-outs.

Creep mechanism is considered to be the most important mechanism of rock glacier movement (e.g., Whalley, 1974) as all other forms of transport discussed above are more – although not exclusively – related to the phase of emplacement and are characterized by short-term events (figure 3.4a,b). In general, material with interstitial ice is subject to slow creep deformation under gravity. Creep occurs also in debris bodies that are free of ice and will move slightly faster as the cementing effect of ice is missing (Johnson, 1987). The process of rock-glacier creep, however, must be separated into creep of a solid ice core and – more importantly – creep of interstitial ice (Giardino and Vick, 1987). Both processes are fairly understood and discussed in detail in, e.g., White (1976); Barsch (1969); Haeblerli (1985). Ice increases the strength of any unconsolidated material but it is also that component which deforms most easily

(Barsch, 1996). Deformation depends on factors such as the applied shear stress and normal stress as a function of thickness, material density, temperature, grain sizes and grain form, type, and size of ice crystals (Barsch, 1996).

Ice is generally considered rheologically as fluid having high viscosities and which deforms under small applied shear stresses until the deformation reaches a permanent value. As the viscosity of ice is not constant but depending on the applied shear stress, temperature and a number of other controlling factors, it is treated as ideal plastic. Polycrystalline ice therefore behaves more as a solid (Paterson, 1981) and if it is considered as perfect plastic, its yield stress is approximately 100 kPa. The relation between strain rate (after peak strain has been reached) and applied stresses is given by Glen's law (Glen (1952), see also Paterson (1994), p. 85f).

$$\dot{\epsilon}_{xy} = A \cdot (\tau_{xy})^n \quad (3.1)$$

where $\dot{\epsilon}_{xy}$ [a^{-1}] is the final strain rate, τ_{xy} [Pa] is the shear stress, A is a temperature-dependent parameter according to the Arrhenius relation * with $A^\dagger = 0.148 [\text{a}^{-1}\text{bar}^{-4.2}]$ and $n = 1.9-4.2$ [-] (Barsch (1996), see also Paterson (1994), p. 86f).

Creep occurs within three strain-rate regimes; the field of secondary creep is the most relevant for glacier and rock glacier dynamics (figure 3.6a). Primary creep rapidly approaches a constant value and the creep rate reaches zero while the field of tertiary creep is steadily increasing. Secondary creep, however, relies on factors such as ice content, temperature, applied stress, load, and characteristics of the soil and is (for rock glaciers) characterized by the following equation

$$\dot{\epsilon} = A\tau_o^m + B\tau_o^n \quad (3.2)$$

according to McRoberts (1975), B , m , n are temperature dependent parameters. The stress at the base of a

* $A = A_o \exp(-Q/RT)$, with A_o being temperature-independent, R being the universal gas constant ($8.314 [\text{J}/(\text{mol}\cdot\text{K})]$), Q [kJ mol^{-1}] being the activation energy for creep, T is the temperature [$^\circ\text{C}$] (see Paterson, 1994, p. 86f).

† Units for parameter A contain "a-bar" which were intentionally not changed to "s-Pa" in this work for compatibility reasons, however, "bar" is still considered to be an SI-conformal unit with $1 \text{ bar} = 1 \cdot 10^5 \text{ Nm}^{-2} = 100 \text{ kPa}$ which translates to A [$\text{a}^{-1}\text{Pa}^{-21}$]

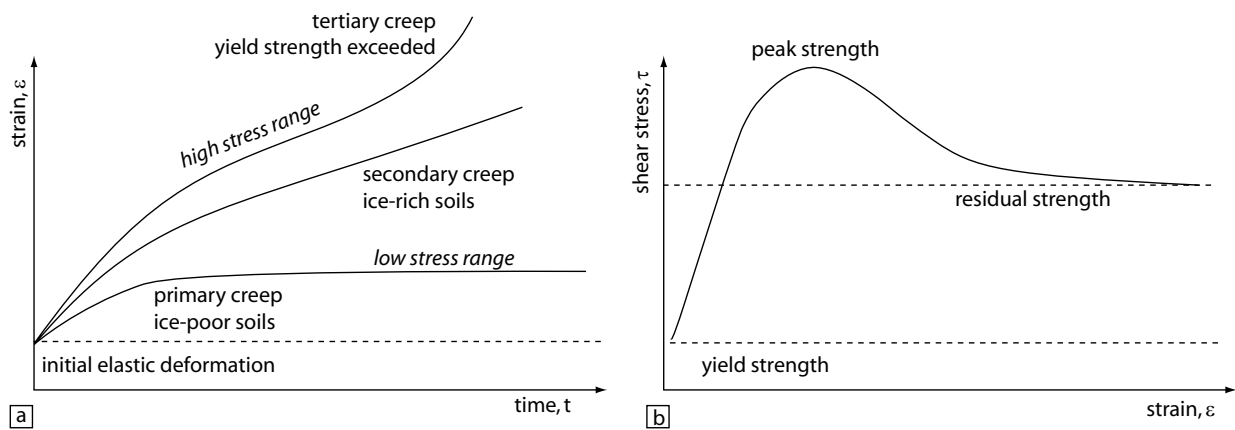


Figure 3.6.: Creep relationships for frozen soils, after *Andersland et al. (1978)* and *Vitek and Giardino (1987)*.

rock glacier is usually calculated by

$$\tau = \rho gh \sin \alpha \quad (3.3)$$

ρ [$\text{kg}\cdot\text{m}^{-3}$] is the density of the material mixture, g [$\text{m}\cdot\text{s}^{-2}$] is the gravitational acceleration, h [m] is the thickness of the rock glacier, and α [$^{\circ}$] is the inclination of the basal plane. Based on this relation, the basal shear stress was calculated to be between 100–200 kPa (*Wahrhaftig and Cox, 1959*), 110 kPa to over 350 kPa (*Haeberli, 1985*) or even far lower than 100 kPa as shown for the Murtel I rock glacier (*Wagner (1992)* as cited in *Barsch (1996)*).

Final strain rates have been calculated by some authors using Glen's law (*Glen, 1952*) obtaining values in the range of 10^{-3} to 10^{-4}a^{-1} (e.g., *Haeberli et al., 1979*; *Haeberli, 1985*; *Wagner, 1992*; *Barsch, 1971*). It was shown that with a sand content above 42%, deformation rate decreases considerably (*Jessberger, 1965*). The reader is referred to works by *Glen (1952)*, and *Goughmour and Andersland (1968)*; *Vialov (1965)* as cited in *Barsch (1996)*, and *Hooke et al. (1972)*; *Roggen-sack and Morgenstern (1978)*; *Haeberli (1985)* for more detailed treatment of the physics of these systems.

As emphasized by *Giardino and Vick (1987)*, main types of movement are creep of an internal ice core or interstitial ice, landsliding and basal shearing. None of the processes should be considered as exclusive process but thus far, not much knowledge has been

obtained regarding the effect of the interaction of such combined processes. The effect of movement is caused by various effects, such as (1) settling of unconsolidated debris masses and filling of voids during resettling, (2) melting of ice, (3) high hydrostatic pressures due to changes in the rock glacier's drainage system, (4) solifluction, i.e., the slow creep of fine-grained surficial debris under gravitational forces, (5) terminal rotational slumps, and (6) deformation of remnant ice blocks (*Johnson, 1987*).

3.1.4.2. Microrelief and Textural Properties

Similar to glaciers but even more akin to lava flows and landslides (*Haeberli, 1985*), rock glaciers host a variety of textural or fine-scaled relief properties summarized as *microrelief*. A rock glacier's microrelief comprises ridges, furrows and pits, all of which have a specific origin and allow inferences on environmental conditions (e.g., *Wahrhaftig and Cox, 1959*; *Barsch, 1996*). Longitudinal ridges and furrows on rock glaciers are generally caused by differential accumulation of debris and snow at the rock glacier's head and involve a complex interaction with melting and persistence of seasonal snow patches as described in *Wahrhaftig and Cox (1959)*.

Transverse ridges and furrows are formed whenever flow of the rock glacier is slowed down or even stopped for some time by, e.g., obstacles or a significant downstream accumulation of debris at the termi-

Table 3.2.: Relationship of rock glacier source areas to surface areas of rock glaciers, where A_S is the area of the source area and A_R is the size of the rock glacier. After (Barsch, 1996).

author	working area	relation
<i>Wahrhaftig and Cox (1959)</i>	Alaska Range	$A_S = 1.36 \cdot A_R + 22.320$
<i>Barsch (1977b)</i>	Swiss Alps, debris rock glaciers	$A_S = 1 - 3 \cdot A_R$
<i>Barsch (1977b)</i>	Swiss Alps, talus rock glaciers	$A_S = 1 - 4 \cdot A_R$
<i>Gorbunov (1983)</i>	Zailiyskiy Alatau Kazakhstan	$A_S = 4.4 - 7.2 \cdot A_R$

nus. The flow is shortened and thus resulting in overthrusting along shear surfaces of debris. Transverse ridges and furrows are bent in downvalley or downslope direction.

In contrast to these, crevasses or tension cracks are widely spaced furrows that form perpendicular to transverse ridges as a result of lateral spreading of the rock glacier. These furrows are comparable to glacial crevasses but in contrast to these, crevasses on rock glaciers are usually filled with coarse debris during further advance. Ridges form due to decelerating flow and are generally caused by (a) differential movement of debris layers (*Ives (1940)* in *Barsch (1996)*), (b) compressive flow (*Wahrhaftig and Cox, 1959; Potter, 1972*) and/or (c) variations in the supply of debris (*Barsch, 1977a*) as summarized by *Loewenherz et al. (1989)*.

While these microrelief forms are fairly common and can be attributed to glaciers as well as rock glaciers other forms are characteristic of rock glacier systems. Among these, isolated or aligned conical pits form when running water melts a tube into the surface which becomes subsequently filled with debris. They form predominantly along longitudinal furrows which form runways for water (*Wahrhaftig and Cox, 1959*). The second and most characteristic feature of rock glaciers are large lobes that form during rock glacier advance after stages of dormancy. These lobes can be considered as individual small rock glaciers on the back of a larger underlying rock glaciers (*Wahrhaftig and Cox, 1959*).

3.1.4.3. Rock-Glacier Geomorphometry

Morphometry is used whenever large amounts of data need to be compiled in order to find characteristic properties of landforms. This method is furthermore of great value when inaccessibility of landforms in the field limit access to data and remote-sensing data has to be used exclusively in order to characterize an area. Although this section is of limited importance for characterizing the nature and behaviour of rock glaciers, it summarizes some of those values obtained during field work and remote-sensing data analysis so that a common base for comparisons to Martian landforms is established.

Morphometrically derived rock-glacier characteristics comprise foremost areal as well as volumetric data of these landforms. Rock glaciers have a length and width of tens to hundreds of meters and a height of 10 m to 100 m at the terminus (e.g., *Barsch, 1996*, p. 22ff). The length of some tongue-shaped landforms can reach over 1000 m at dry mountainous locations (650 m in San Juan Mountains, Colorado, up to 2100 m in the Brooks Range, and up to 6000 m in Greenland (*White, 1979; Calkin et al., 1987; Humlum, 1982*)). Thicknesses of tongue-shaped rock glaciers are in the range of 20 m to 200 m (*Barsch (1996)* and references cited therein).

Lobate rock glaciers are considerably shorter, they usually reach a maximum length of 400 m and a thickness of up to 30 m with a length to thickness ratio of approximately 3:2 (*Barsch (1996)* and references cited therein). Thickness, however, can usually only be sufficiently well determined using geophysical experiments but is often estimated based on the

height of the terminus. Maximum thicknesses for lobate rock glaciers are in the range of a few tens of meters (80 m as determined by *Calkin et al. (1987)*).

It is plausible that the size of the rock glacier is directly connected to the size of the source area: the more material is provided, the larger the rock glacier will be. *Barsch (1996)* summarizes that this observation is confirmed by field measurements from the Brooks Range where cirque walls have a height of up to 250 m (*Ellis and Calkin, 1983; Ellis et al., 1983*) and rock glaciers are up to 110 m thick (*Barsch, 1996*, p. 29). Few authors have provided values for this relationship that is summarized in table 3.2. It must however be kept in mind that these values have their natural limitations and that rock glacier development, especially if it is subject to long-term development, has undergone various climatic changes that are not represented by such numbers. For further reading and details about geomorphometric measurements beyond the work summarized herein, the reader is referred to *White (1979)* and his work carried out in Colorado area.

3.1.5. Summarizing Comments

The previous sections attempted to summarize some of the most relevant aspects of terrestrial rock glacier systems that need to be discussed in order to compare these features with possible Martian systems discussed hereafter (section 3.2). The above summary is far from being complete and should be considered as entry point for further work cited therein. It has been shown, that many aspects of rock glacier research are not clearly understood, starting with alleged simple morphologic descriptions and definitions and ending with the physics of these systems and the behaviour of ice and debris under varying environmental conditions. Even with a considerable knowledge gained through field work, some of the observed features are still controversially discussed. The variability of the structure of rock glaciers and the different appearances of ice within such a debris-transport system make it obviously complicated to find a common base for discussion, and measurements in the laboratory

do often not represent the true conditions. More details on such problems are summarized and discussed in *Barsch (1996)*.

3.2. Martian Landforms related to the Creep of Ice and Debris

In this section a summary of work on Martian creep-related landforms is provided by covering the nature and evolution of (a) lobate debris aprons and associated morphologic features (i.e., concentric crater fill and lineated valley fill) in section 3.2.1, (b) viscous flow features in section 3.2.2, and (c) the so-called fan-shaped deposits of Martian equatorial latitudes in section 3.2.3. Although the latter are considered to be of glacial origin by most authors, morphologic similarities to rock glaciers indicative of permafrost environments justify a short summary on these landforms also. The amount of literature covering various research foci at different locations on Mars as well as a highly inconsistent nomenclature require additional in-depth discussions on these topics; therefore, the following sections are separated according to different research aspects and are presented as summaries in a chronologically consistent view to account for the different approaches made by various research groups.

3.2.1. Lobate Debris Aprons and Associated Landforms

Among a rich variety of landforms on Mars that are connected to mass-wasting processes, such as landslides, avalanches or rock-fall morphologies, the so-called *lobate debris aprons*, *lineated valley fill* and *concentric crater fill* features are the most prominent landforms that are not only attributed to mass-wasting but that are also connected to processes related to permafrost and periglacial environments (*Carr and Schaber, 1977; Squyres, 1978, 1979; Lucchitta, 1981*). Although these landforms can have a remarkable size and have been investigated in detail on the basis of Viking image data already (figure 3.7), several questions regarding their origin and evolution are being still discussed and a connection between

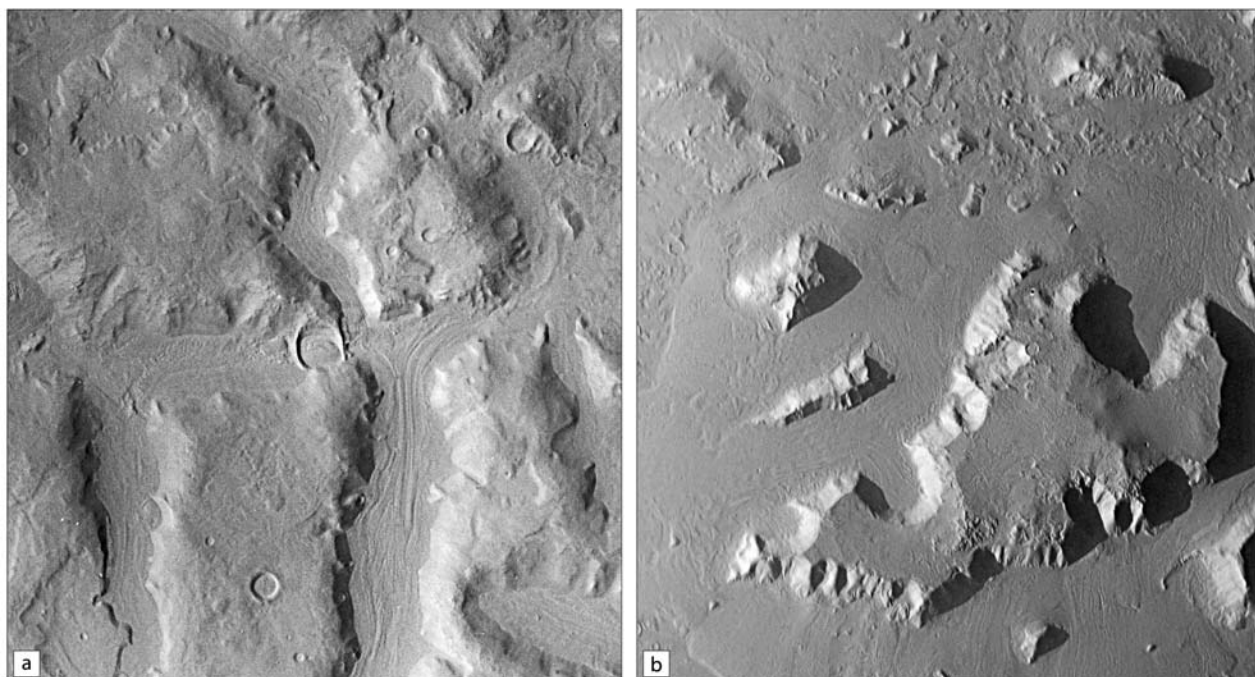


Figure 3.7: Type locations of debris aprons and related landforms in northern Arabia Terra, [a] lined valley fill in Nilosyrtis Mensae at 70°E , 34°N , scene width is 40 km, Viking orbiter frame Fo84A73, 38 m/px; [b] lobate debris apron in Protonilus Mensae, 48°E , 47°N , scene width is 81 km, Viking orbiter frame Fo58B55, 77 m/px. Illumination in both scenes from left.

various locations on Mars has not been established thus far. Except for very few alternative explanations (e.g., *Malin and Edgett, 2000*), it is generally accepted that lobate debris aprons and related landforms are the result of creep and deformation of ice-rich debris masses and compare closely to terrestrial rock glaciers (*Carr and Schaber, 1977; Squyres, 1978, 1979; Lucchitta, 1981*).

3.2.1.1. Shape and Characteristics

Footslopes of buttes and mesas located near the northern highland-lowland boundary escarpment are characterized by broad so-called lobate debris aprons that are considered to represent macro-scale systems of debris-ice transport systems at Martian mid-latitudes. Lobate debris aprons usually have a well-defined upward-convex longitudinal profile with a generally flat mid-slope and a steep terminus. In top-view, lobate debris aprons extend away from remnant massifs and escarpments forming multiple lobes.

Each of these lobes show characteristic patterns of concentric and/or radial ridges and furrows indicating compressional and extensional deformation suggestive of creep of ice and debris.

Lobate debris aprons can reach a length of a few hundred to several thousands of meters and reach an apparent thickness of tens to hundreds of meters. In areas of dense occurrences and clusters of lobate debris aprons, aprons often coalesce and form complex overlapping lobes of debris masses which originated from multiple source remnants. This view was presented in Viking image data with relatively coarse spatial resolution. Consequently, first work on lobate debris aprons as performed by *Carr and Schaber (1977); Squyres (1978, 1979)* focused on the general shape, the global distribution, and some speculations about the origin of these landforms.

Lobate debris aprons are generally lined either perpendicular, i.e., radially outward, or parallel to the escarpment faces and are suggestive of viscous de-

formation (*Squyres, 1978*). As for terrestrial rock glacier analogues (*Wahrhaftig and Cox, 1959*), longitudinal lineations are believed to be caused by inhomogeneities in the supply of debris or a heterogeneous distribution of ice causing variable flow rates. In contrast to this, transverse ridges, i.e., ridges perpendicular to the main flow direction, are commonly considered to be caused by obstacles that blocked advance of debris movement (see also section 3.1.4.2). The case for lineated valley fill lineations is slightly different according to *Squyres (1978)*. Valley-parallel alignments of lineations would theoretically speak for a direction of debris transport along valley (i.e., flow lines) but the valley termini lack any depositional features. Furthermore, if these lineations would be flow lines, the opposite terminus of lineations must point towards the source of debris supply. This configuration could not be observed. *Squyres (1978)* interpreted such valley floor lineations as compressional features that are formed when debris originating at valley walls is transported towards the center of the valley. After the valley was filled and flow was diverted (*Squyres, 1978*), additional ridges might have formed that are also aligned in parallel direction to the valley walls and which are derived from along-valley movement of debris. At closer inspection, some of the lineations are more akin to aligned pits rather than real furrows or ridges which *Squyres (1978)* explained as possible collapse pits caused by evaporation and subsequent deflation of material.

Lucchitta (1981) summarized these earlier observations by *Squyres (1978, 1979)* and additionally discussed debris apron landforms found at equatorial latitudes, such as the western lobes at Olympus Mons. *Lucchitta (1981)* compared a broad lobe with the similar-looking terrestrial Malaspina piedmont glacier, and compared more elongated lobe features at Olympus Mons with rock glaciers in the Wrangell Mountains. This view was later revived in *Head et al. (2005)* and will be discussed in more detail in section 3.2.3. Moraine-like ridges found at the western part of Arsia Mons and also in Utopia Planitia were compared to terrestrial recessional moraines. However, *Lucchitta (1981)* did not explicitly state that these

landforms are of glacial origin but she confirmed using a variety of terms ranging from *glacier-like flow*, to *rock glacier* and *debris flow*, that creep of debris and ice might have been involved in the formation of such features. Due to their broad lobate shape, other terms, such as piedmont aprons (*Lucchitta, 1981*), have been proposed but did not find their way into literature.

3.2.1.2. Distribution and Occurrences

Lobate debris aprons are predominantly located at Martian mid-latitudes either at the northern-hemispheric dichotomy boundary or at the southern-hemispheric impact-basin margins (figure 3.8). Their occurrence at the northern hemispheric dichotomy boundary is connected to the so-called fretted terrain, an area that was first discovered and described by *Sharp (1973)* on the basis of Mariner 9 image data and also by, e.g., *Carr and Schaber (1977)* discussing possible flow features on Mars.

The Martian fretted terrain is characterized by a degradational band between the intact southern highland terrain and the northern hemispheric lowlands. Dissection and degradation of the highland increases towards the north so that the transition zone between both large-scale physiographic units is characterized by a southern zone of intact highland terrain, an intermediate zone of dissected highland plateaus and broad fretted channels, and a northern zone with occurrences of isolated remnants and mesas (figure 3.8). According to *Sharp (1973)*, the upland plateaus could be composed of thick regolith containing substantial amounts of ice, a view that was later also supported by *Malin (1975)* (as cited in *Squyres (1978)*), *Carr et al. (1976)* and *Carr and Schaber (1977)*. Formation of the dichotomy escarpment was considered to be caused by recession of the highland terrain and release of ground water and ice towards the northern lowlands (*Sharp, 1973*), a view that has become relatively unpopular in more recent investigations using MOLA topographic data. There seem to be, however, two processes that interact: the first one is related to the formation of the dichotomy-boundary escarpment in early Martian history, the

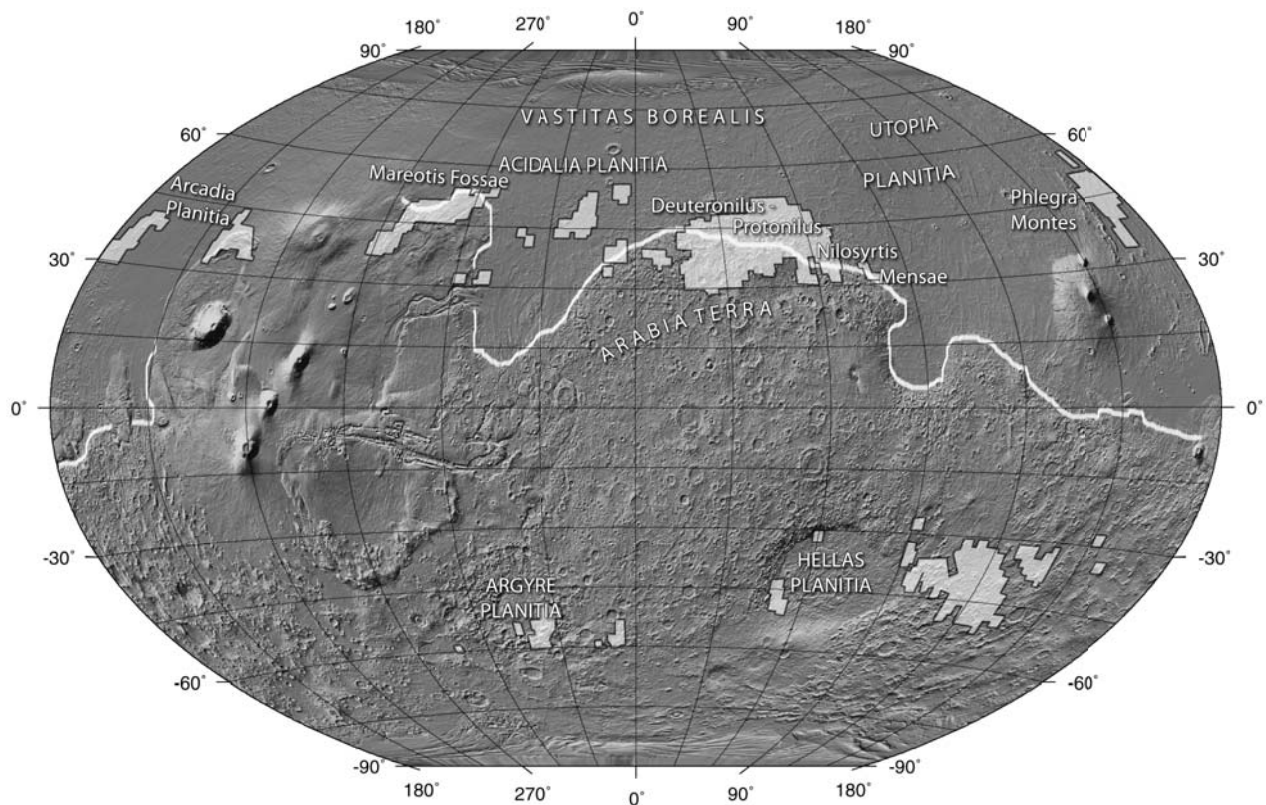


Figure 3.8.: Approximate locations of areas with high densities of occurrences of flow features (lobate debris aprons, lineated valley fill and concentric crater fill) as identified by *Squyres (1979)* (filled white areas), digitized and re-projected using figure in *Squyres et al. (1993)*, p. 543. Shaded relief from MOLA topographic gridded data records, PDS. White line marks approximate location of the dichotomy boundary. Compare also with figure 12.6 in chapter 12, p. 183 on *Geomorphic Evidence for former Lobate Debris Aprons at Low Latitudes on Mars: Indicators of the Martian Paleoclimate*.

other one is characterized by the disintegration of that boundary escarpment due to processes discussed hereafter. Lobate debris aprons, lineated valley fills and concentric crater fills described by *Squyres (1978, 1979)*; *Squyres and Carr (1986)*; *Carr (1987)*; *Squyres (1989)* are accompanied by a generally smoothed topography that indicates resurfacing processes which caused obliteration of any fine-scaled features and was termed "terrain softening" (figure 3.9).

Squyres (1979) mapped the global distribution of debris aprons and related landforms initially observed by *Squyres (1978)* on high- to intermediate-resolution Viking image data. He found out that debris aprons and related features indicative of flow are distributed along two hemispheric bands, each 25° wide and centered at 40°N and 45°S. These regions are the fretted

terrain areas of Deuteronilus, Protonilus and Nilosyrtis Mensae, the eastern and western parts of Acidalia Planitia, Mareotis Fossae, an arc north of Olympus Mons, and the Phlegra Montes. The concentric crater fills, first mentioned in *Squyres (1979)* are located predominantly in the Utopia Planitia region. The southern hemisphere shows occurrences of debris aprons at the Argyre and Hellas Planitiae rims (see figure 3.8).

The latitudinal distribution of lobate debris aprons and related landforms suggests a climatic control and areas of high annual H₂O frost deposition as proposed by *Squyres (1979)*. This view was initially confirmed by earth-based spectra and Viking Orbiter as well as Viking Lander observations of long-term frost deposition in the northern lowlands (*Barker, 1976*; *Farmer et al., 1977*; *Jones et al., 1979*).

EXCURSION: THE MARTIAN DICHOTOMY BOUNDARY

Tharsis and Elysium as well as the large impact basins Argyre and Hellas Planitiae are some of the most prominent physiographic features of the Martian surface. In the northern hemisphere, a steep escarpment spans the Martian surface which separates the northern lowlands from the southern highland terrain (*Mutch et al., 1976; Carr, 1981*). The southern highlands make up approximately 65% of the Martian surface while the northern lowlands occupy the other third (*Pepin and Carr, 1992*). Apart from this physiographic boundary, the highland shows a much higher impact crater density than the smooth lowlands indicating a much younger age of the northern hemispheric lowlands.

Although the global dichotomy could be detected in early Mariner image data, the height of the escarpment of about 3 km could only be approximated photogrammetrically using Viking image data. Later, this value was confirmed by high-precision laser altimeter tracks from the MOLA instrument. The bimodal distribution of binned topographic heights shows that the lowlands are 5-6 km lower than the southern highlands (*Aharonson et al., 2001*). The cause of this global dichotomy still remains unknown. The global dichotomy escarpment is one of the oldest structures on Mars dating back to >3.8 Ga in the early Noachian when the high-impact flux slowly ceased (*Pepin and Carr, 1992; Schubert et al., 1992*). It is generally assumed that the area of the dichotomy boundary was exposed to resurfacing processes until the Hesperian (*Scott and Tanaka, 1986; Greeley and Guest, 1987*). One theory says that the possible reason for this dichotomy is found in a giant impact event (*Wilhelms and Squyres, 1984; Frey and Schultz, 1988; Pepin and Carr, 1992*) that took place in the northern lowlands. Other theories favour large-scale mantle convections that have built up the southern highlands during planetary accretion processes (*Wise et al., 1979a,b; Davies and Arvidson, 1981; Hess and Parmentier, 2001*). A third theory considers plate tectonics as a main process for shaping of the boundary (*Sleep, 1994; Connerney et al., 1999*). The MOLA instrument onboard Mars Global Surveyor has shed some light on this issue and it is assumed that the difference between the center of mass and the body center causes the dichotomy effect (*Albee et al., 2001*).

Beside this, it is assumed that topographic differences are caused by large-scale differences in crustal thicknesses: the dichotomy boundary might be a result of Tharsis-related volcanism, crater-impact events in Isidis and possibly Utopia Planitiae, as well as modification by fluvial processes and outflow events in the circum-Chryse Planitia region (*Smith et al., 1999*). Spectral data from the Thermal Emission Spectrometer (TES) onboard Mars Global Surveyor shows that the northern lowlands are composed of andesitic rocks while the southern highlands are mainly composed of basalts (*Christensen et al., 2001*).

For a recent treatment of the development of the Martian dichotomy boundary and an extensive review the reader is referred to *Watters et al. (2007)*.

Two observations regarding the global distribution of LDA remain however unresolved, one is the latitudinal difference as documented by a high abundance of these landforms in the northern hemisphere and only few occurrences in the south, the other one is a variation in the longitudinal distribution of debris aprons although factors such as elevations and ages (*Soderblom et al., 1974*) are comparable. The patchy

distribution is explained by *Squyres (1979)* by differences in material composition, consolidation and material strength which result in higher erosion rates in the north. Although plenty of escarpments capable of providing eroded material are observed in the south, not all of these show debris aprons at their footslopes. Other explanations by *Squyres (1979)* put forward higher frost deposition rates at the impact

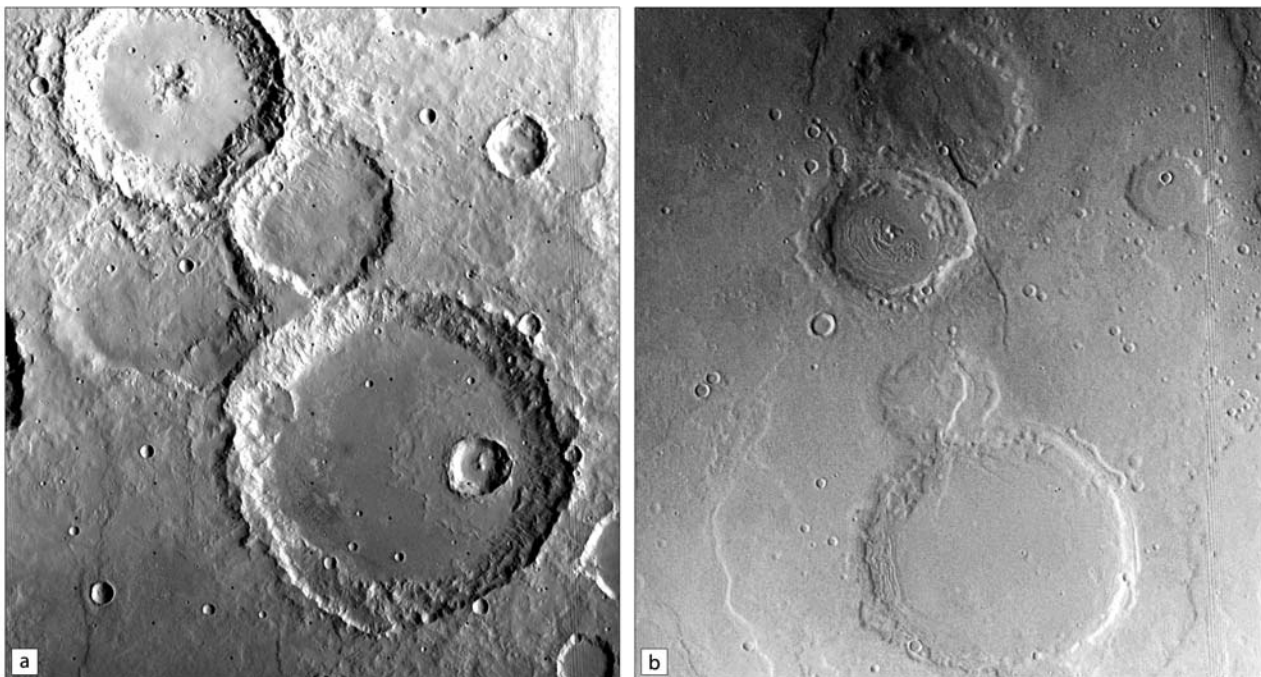


Figure 3.9.: Terrain softening as visible at impact craters, [a] rough terrain showing crater with sharply defined crests and rims at 133°E , 32°S , scene width is 150 km, Viking orbiter frame 423S10, 117 m/px; [b] so-called softened terrain showing craters with smoothed rims at 47°E , 33°N , scene width is 60 km, Viking orbiter frame 195S20, 47 m/px. Illumination from the lower right [a], and from the left [b].

basins to explain longitudinal differences. As summarized by *Squyres and Carr (1986)*, the distribution of landforms suggests that ice at low latitudes is not in equilibrium with the atmosphere and has therefore been lost by processes such as sublimation or diffusion through the regolith, thereby causing a net poleward transport of ice in Martian history.

The latitudinal control of the distribution of lobate debris aprons and related landforms may also be caused by the presence and stability of ground ice as well as changes in the rheological behaviour of ice at different latitudes and consequently at different temperatures. While in areas equatorwards of 30° latitude north and south, ice is not stable at the near subsurface and tends to escape via sublimation or diffusion, it becomes stable between $30\text{-}55^{\circ}$. Beyond that, the viscosity is increased for temperatures between 160-200 K and creep is not facilitated anymore.

An alternative that was proposed by *Lucchitta (1984)* and which was adopted by *Squyres and Carr (1986)*

suggests that climatic changes due to obliquity cycles on scales of 1.2×10^5 years are responsible for changes in the stability of near-surface ground ice causing cycles of deposition and removal of ice at different latitudes.

3.2.1.3. Nature and Origin

Nature and origin of flow features at the fretted terrain have been briefly discussed by *Carr and Schaber (1977)* who suggested mechanisms such as frost creep or gelifluction. *Squyres (1978)* disagreed with this idea for two reasons, one was the considerable thickness that is affected by creep deformation, the other one was that there is no evidence for thawing of material to a considerable depth which would favour gelifluction of an upper layer. The relatively fresh appearance of these flow features would require thawing in recent times which would not be possible under current climatic conditions and, e.g., volcanic heat sources are excluded for reasons of lack of vol-

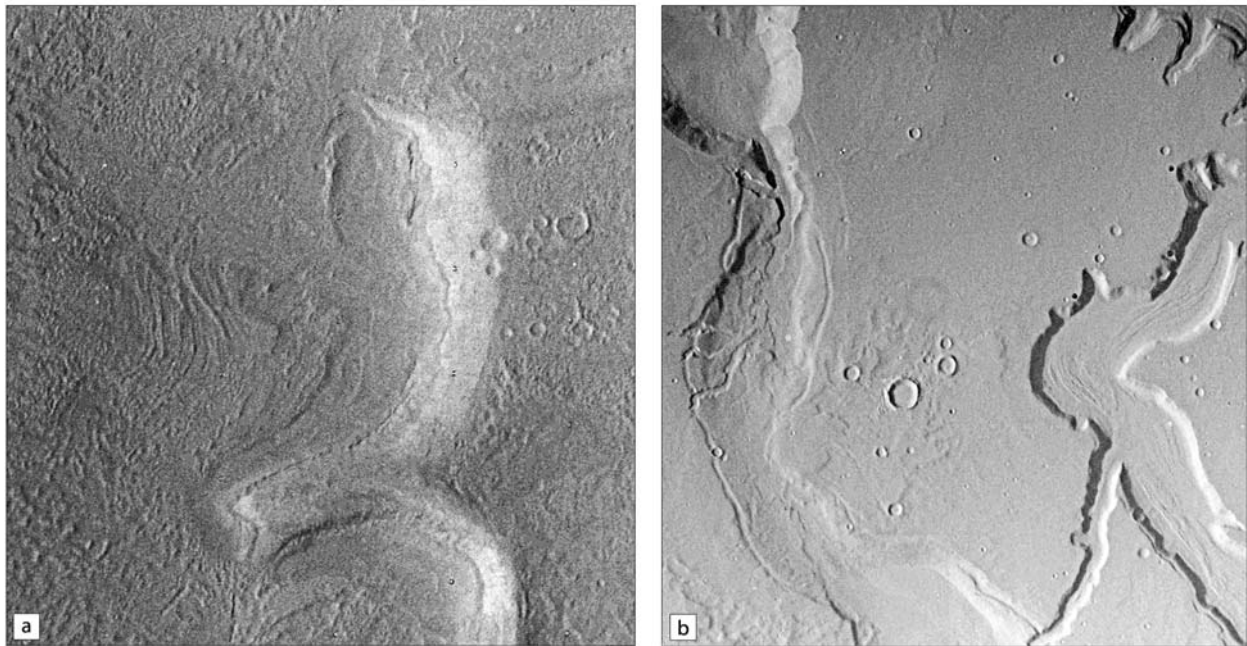


Figure 3.10.: Degradation landforms at the Fretted Terrain (FT). [a] collapsed channels indicating removal of ground ice in Deuteronilus Mensae at 14.2°E , 44.8°N , scene width is 5.6 km, Viking orbiter frame F458B46, 10 m/px, illumination in both scenes from upper left. [b] disintegrated debris surface with pits and hollows indicating thermokarst-like degradation processes 16.3°E , 33.2°N , scene width is 16.3 km, Viking orbiter frame 637A16, 49 m/px. Illumination in both scenes from upper left.

canic features in the vicinity (Squyres, 1978). Instead, Squyres established a connection to other terrestrial periglacial processes and suggested a formation more akin to terrestrial rock glaciers where creep occurs through the deformation of ice and debris rather than through melting of ice (e.g., *Wahrhaftig and Cox, 1959*). The source of ice as suggested by Squyres (1978) was considered to be direct atmospheric condensation or outgassing connected with freezing although quantitative estimates could not be provided at that time. This view has later been revived and given preference over the idea that the possible source of water and ice is related to highland erosion (Squyres and Carr, 1985; Squyres and Carr, 1986). The source of debris is even more uncertain and Squyres considered flow of material collected at the footslope in the course of highland erosion as a possible mechanism. Although Lucchitta (1984) generally agreed with the theory of ice-lubricated flow of debris, she disagreed about the source of ice and the climatic control sug-

gested by Squyres (1978). According to Lucchitta (1984), frost would be far too unstable to percolate into talus debris as shown at the Viking Lander 2 site (Utopia Planitia, 134.2°E , 48°N). In order to preserve frost, it must have been buried quickly which again would have caused dilution and would therefore prohibit lubrication. The alternative presented by Lucchitta (1984) is derivation of ice from underground as supported by observations of numerous collapse structures and collapsed channels in the surroundings (figure 3.10). Lucchitta suggested that volcanic cap rocks might have played a role during formation of debris aprons as subsurface ice would have caused flow of debris and smoothing of relief which is not observed. Lucchitta (1984) proposed that ice might have filled pore space but has not weakened the strength of rock material substantially to allow flow. Subsequent oversteepening of scarps could then have caused disintegration and weakening of rock material (Lucchitta, 1984). Lucchitta also suggested, that

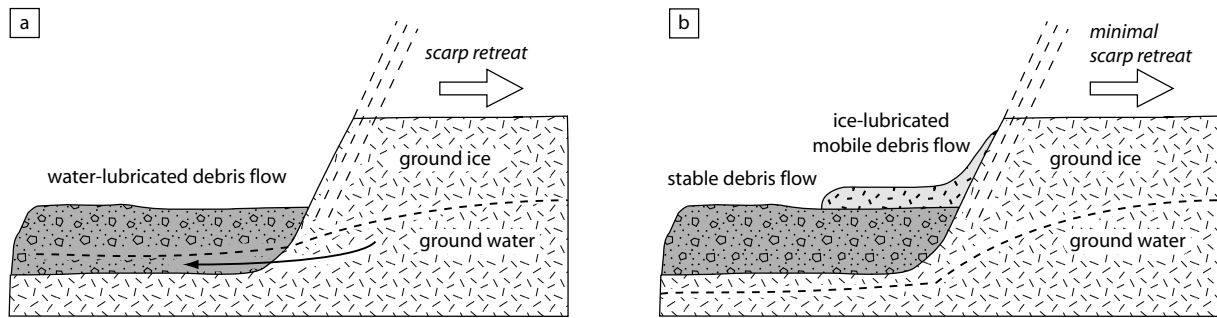


Figure 3.11. Two-stages model of debris apron and lineated valley fill formation. [a] ground water lubricated debris collects at footslope, headward erosion provides debris input. [b] after northward movement of the 273 K isotherm water freezes and debris movement ceases. Ice-lubricated debris collects on top of debris base. Modified after (Carr, 1995).

an amount of 10% of ice would have been enough to weaken the material, similar to landslide liquefaction, and that the maximum observed apron lengths of about 20 km were caused by thinning of debris material, loss of ice and decrease of slope angles.

Questions regarding the process responsible for apron formation as well as formation of the fretted terrain remained still open over one decade later. Carr (1995) re-discussed alternatives but left open if debris aprons might still be forming today as suggested by Squyres (1978) or whether they might have reached an equilibrium that prohibits further growth. He concluded that the process for degradation of the fretted terrain could not be responsible for debris apron formation as (a) eroded material from the fretted terrain had been transported much larger distances than the maximum distance of 20 km observed for lobate debris aprons, and (b) scarps must have retreated greater distances than implied by observations. Carr (1995) agreed with Lucchitta (1984) by saying that not all lineations in lineated valley fills are formed by wall-rock debris merging near the center of the valley but that these lineations are also longitudinal striae formed by downvalley transport. He also agreed with Lucchitta that mass wasting alone could not be responsible for formation of debris aprons and lineated valley fills but that material must have been removed from underground as well.

In contrast to the erosion process mentioned above,

the fretted terrain is supposed to have formed as consequence of planation processes (Sharp, 1973; Carr, 1995). Carr (1995) and Carr (2001) considered sapping and headward erosion as mechanism for formation of the fretted-terrain valleys. Along with changing of environmental conditions (heat loss, climate change) the 273 K isotherm might have moved towards the north resulting in stabilization of the water-lubricated mass-wasting debris (figure 3.11).

In contrast to lobate debris aprons and lineated valley fills there was less consensus regarding the nature of concentric-crater fill landforms. Squyres initially puts concentric crater fill into the group of debris apron-related landforms because of some morphological similarities and a spatial distribution comparable to that of lobate debris aprons and valley fill (Squyres, 1989; Squyres et al., 1993). An alternative explanation for formation of concentric crater fills was put forward by Zimbelman et al. (1989) who suggested that these landforms are aeolian deposits. He argued that layering observed with some concentric crater fill deposits in Utopia Planitia is well preserved which would not be the case if the material was subject to slow creep deformation. Squyres et al. (1993) conceded that ice-related deformation as well as aeolian processes might have formed such deposits at some locations on Mars.

In connection with extensive Viking-based geological mapping efforts during the mid 1980s and early 1990s

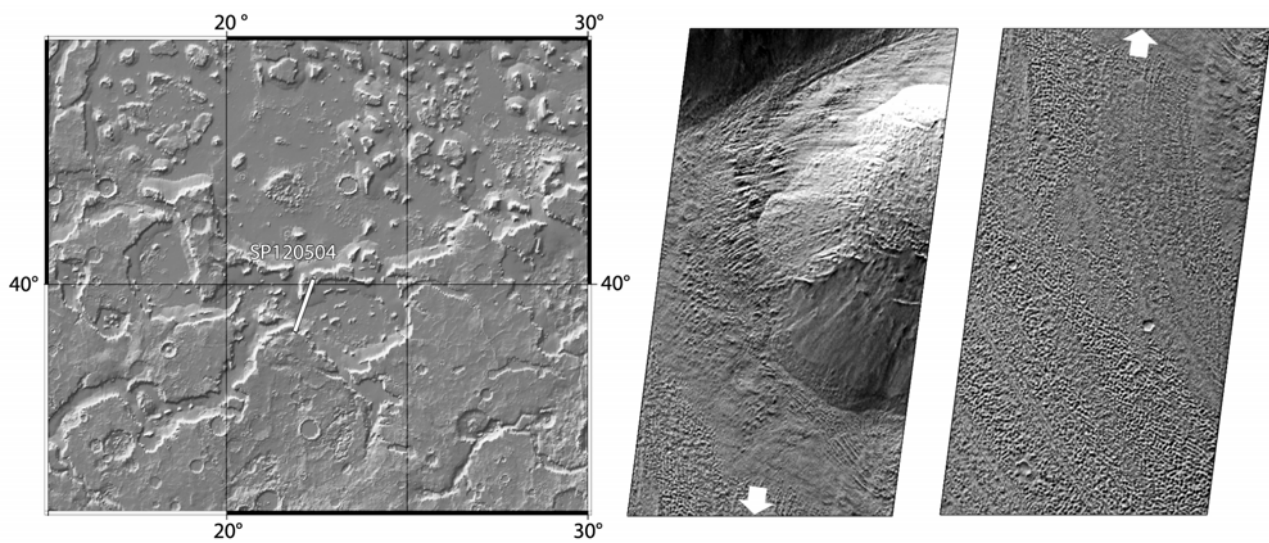


Figure 3.12.: Sample MOC-NA SP12/0504 scene and overview map of a debris apron in Deuteronilus Mensae. Image strip has been cut for display reasons, the northernmost section is to the left. The pitted parallel striping pattern seen on the apron (right) was interpreted as pediment layers rather than flow ridges by *Malin and Edgett (2000)*.

by a group at Arizona State University (ASU), southern hemispheric type areas of lobate debris aprons were revisited and analyzed in detail (*Crown et al., 1990; Greeley and Guest, 1987; Crown et al., 1992; Crown and Greeley, 1993*). Most of the remnant material east of the large outflow channels Dao and Niger Valles (eastern Hellas Planitia) were considered to be Noachian-aged mountainous remnants forming either ejected impact- or uplifted ancient crustal material. These remnants pierce through Hesperian to Amazonian volcanic plains emplaced by the circum-Hellas volcanic constructs such as Thyrrena and Hadriaca Paterae (*Crown et al., 1990, 1992; Mest and Crown, 2001*). Geologic mapping results supported the ideas of *Squyres and Carr (1986)* regarding a rock glacier origin for the Amazonian-aged lobate debris aprons.

More detailed work on debris aprons around Hellas Planitia have been performed by *Crown and Stewart (1995)* by focusing also on the distribution and formation. *Crown and Stewart (1995)* investigated 27 features, either lobate debris aprons or crater fill units and concluded that these homogeneously distributed aprons form in-situ due to slope instabilities

and have neither been transported nor redeposited by aeolian or fluvial processes. They also state that material was at least partly fluidized, either by ice or by water, and that emplacement on top of a variety of Noachian to Amazonian units suggests that these features form one of the youngest units in the area. A variety of subsequent work on the geology of the circum-Hellas Planitia region have supported this view (*Mest and Crown, 1997; Crown and Mest, 1997; Stewart and Crown, 1997; Mest and Crown, 2001*).

Since the end of the 1990's, Mars Global Surveyor has contributed a considerable amount of data that was analysed and which revived debris-apron research by providing very high resolution image data from the Mars Orbiter Camera (MOC-NA) and high resolution altimetry data from the Mars Orbiter Laser Altimeter (MOLA) allowing us for the first time to conveniently extract topographic profiles that are based upon direct measurements. First work on the basis of MOC-NA image data in combination with MOLA topographic data was presented by *Malin and Edgett (2000)* who put forward a completely new hypothesis on debris apron formation (figure 3.12). *Malin and Edgett (2000)* interpreted the pitted striping

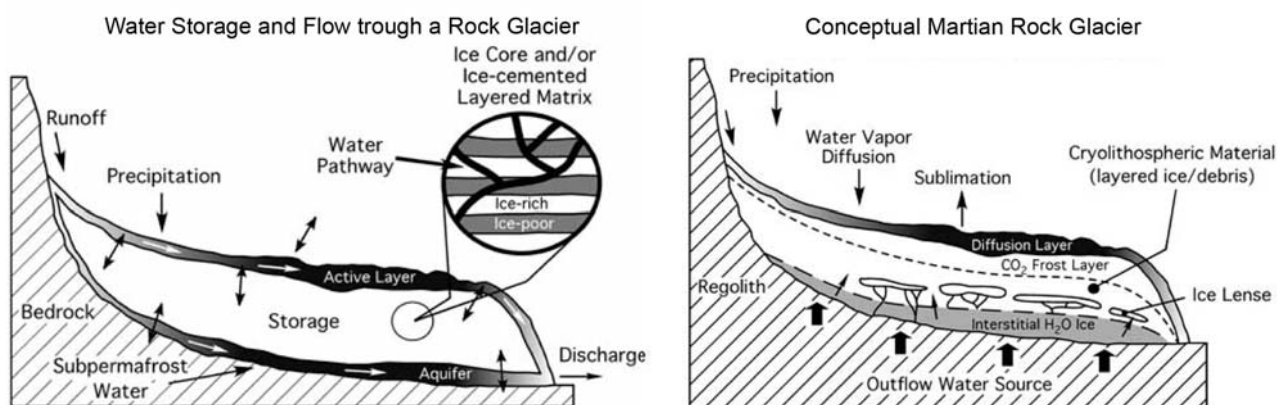


Figure 3.13.: Distribution and flow of water in a terrestrial rock glacier (left) and a Martian debris apron (right), modified from *Degenhardt and Giardino (2003)*.

seen on debris aprons (called *circum-mesa apron*) as bedrock pediments with different materials exposed as different layers. While the upper apron is more pitted and thus experiencing extension (or more intense erosion), the narrow pit pattern at the lower slope would indicate compression or less intense erosion. Although *Malin and Edgett (2000)* could image several areas showing also flow, they doubt that such flow processes would reach any considerable depths as suggested by *Squyres (1978, 1979)*. Their view has, however, not experienced much popularity in subsequent work.

In the post-Viking era, only few publications have contributed to a much more detailed understanding of lobate debris apron formation or have added significant new theories. Most of the early theories that were put forward on the basis of Viking data have now been confirmed with the help of new image data and many type locations have been characterized in more detail.

Post-Viking research foci were put predominantly on (a) a re-investigation of early deformation theories with the help of topographic data, and (b) evidences for thermokarstic erosion processes indicating decay of these landforms. Although there is currently little doubt that lobate debris aprons and associated landforms are indeed rock glacier analogs, several questions still remain open: (1) the nature of lineations in

lineated valley fill deposits, i.e., direction of transport, (2) the volume of ice incorporated in aprons and valley fill deposits, (3) the connection to climate change, and (4) the rheology of debris/ice material (e.g., *Hamlin et al., 2000*). These are by far not the only open issues that need explanations, as, e.g., the timing event still remains unanswered and the mechanism of debris incorporation, i.e., landslide vs. rock fall, is also unclear. *Hamlin et al. (2000)* showed that even with highest-resolution MOC-NA image data it is not easy to prove that lineated valley fill does not only show a flow direction perpendicular to the valley walls as suggested earlier but that there is also a down-valley component of flow. They summarized the sequence of events in the following way: (1) debris accumulation and formation of talus deposits below slopes, (2) enrichment of talus debris with ground ice and contributions from condensing atmospheric water, spring discharge from local aquifers, and ice from plateau-forming materials that are forming the observed talus deposits; (3) formation of interstitial and lenticular ice and deformation akin to terrestrial rock glaciers (*Hamlin et al., 2000*).

For the lineated valley fill, *Hamlin et al. (2000)* suggested that first, ice and debris accumulated below wallrock, then moved perpendicular to valley walls and, as soon as the volume increases, a down-slope component of transport was added. Flow is

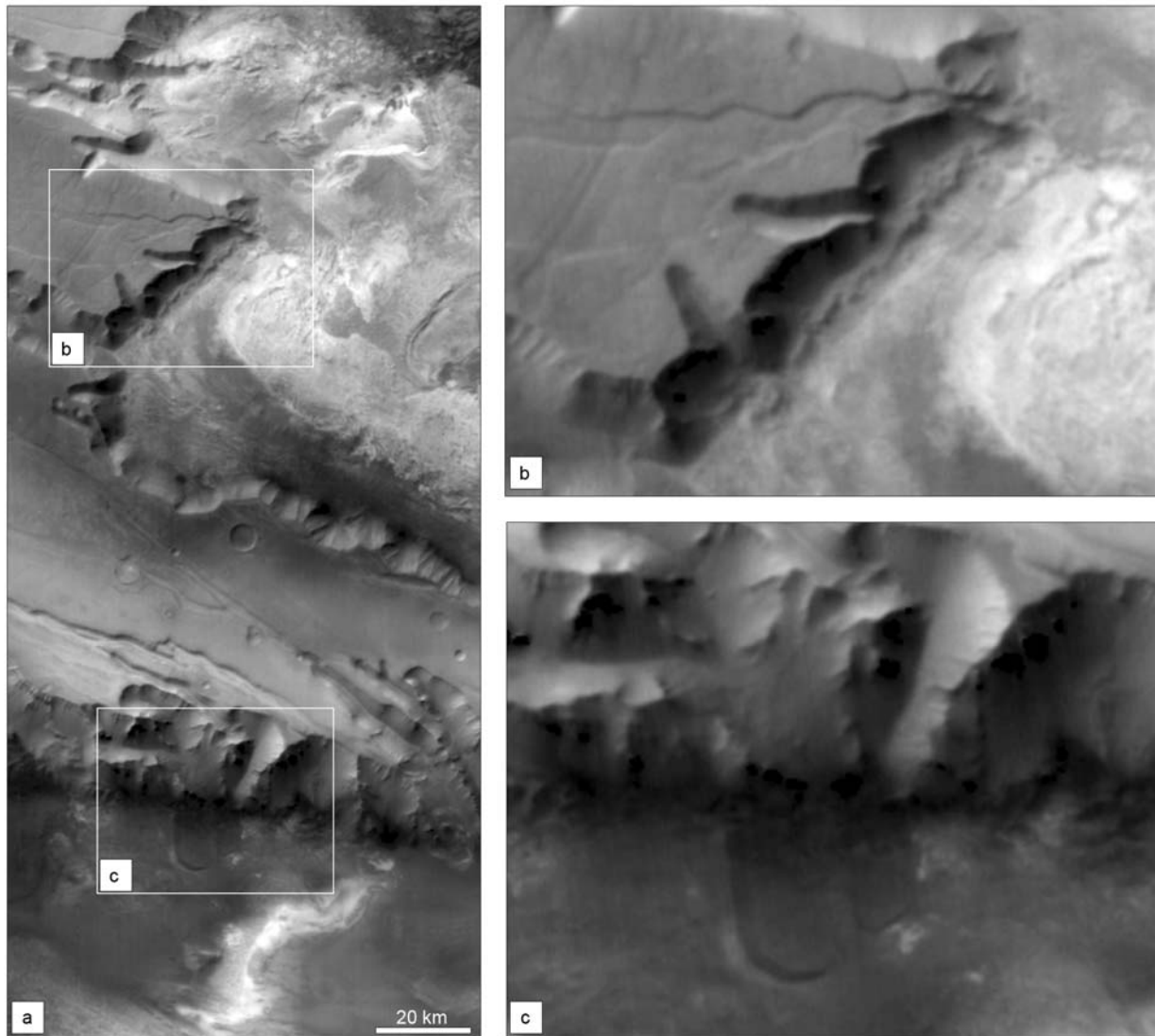


Figure 3.14.: Equatorial Martian landforms suggestive of formation similar to terrestrial rock glaciers and protalus features as interpreted by *Whalley and Azizi (2003)*, MOC-WA FHA01275, location at 283°E , 6.90°S , Ius, Melas, Candor Chasmata, pixel scale 241.1 m/px; see also figure 3.15.

thought to occur through either solid-state deformation or through periodic freeze-thaw cycles similar to gelifluction processes. Preliminary analyses using MOLA topography data showed that slope angles of Martian debris aprons are less steep than those of terrestrial rock-glaciers with values around $1\text{-}2.5^{\circ}$ (see also *Carr, 2001*) on the main flow and $4\text{-}7^{\circ}$ at the terminal parts while terrestrial systems usually show values in the order of 45° at the terminus and $5^{\circ}\text{-}10^{\circ}$ on

the main flow. This discrepancy would probably indicate a different flow regime of Martian debris systems (*Pierce and Crown, 2001; Crown et al., 2002*). In addition, *Crown et al. (2002)* and *Crown et al. (2003)* measured area sizes and volumes of 68 aprons in eastern Hellas Planitia. Results give apron-lobes sizes in the range of $25\text{-}3014\text{ km}^2$ ($6\text{-}4035\text{ km}^2$ in *Crown et al. (2003)*), averaging at 505 km^2 (538 km^2) with a total area occupied by debris aprons of $34,351\text{ km}^2$. Vol-

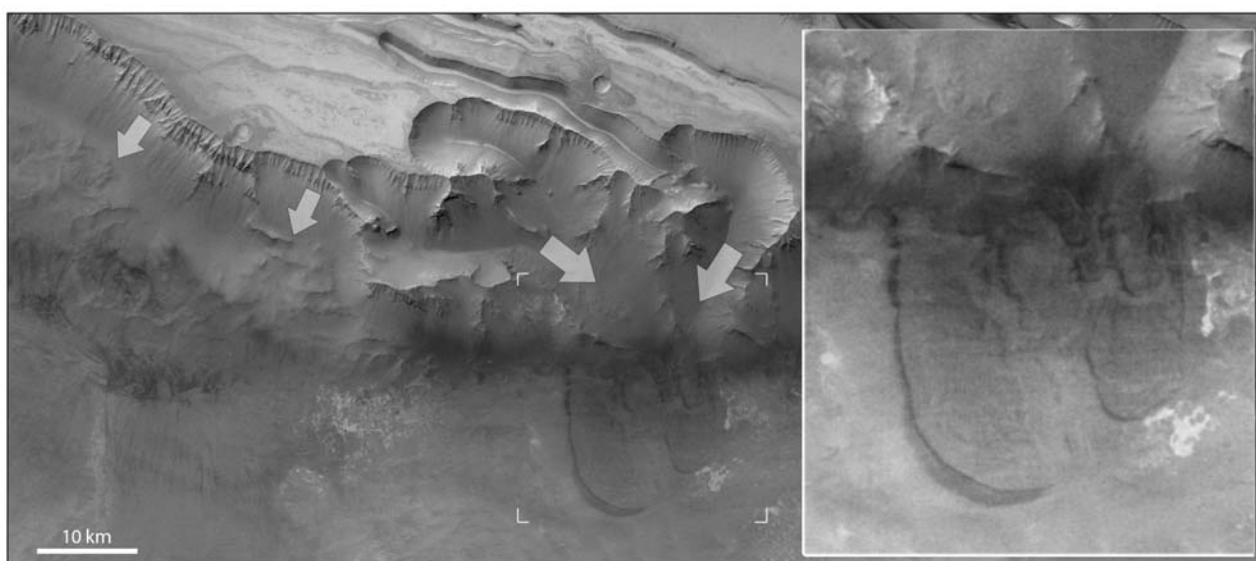


Figure 3.15.: Tongue-shaped feature on the floor of Valles Marineris, see figure 3.14 interpreted as possible rock glacier (*Whalley and Azizi, 2003*). The shape of lobes, central fracture, missing ridge and furrow pattern, flat and unstructured surface, and connection to termini of graben-like incisions suggest a landslide origin rather than that of a rock glacier; HRSC scene 1235, location at 283°E, 7°S.

umes are in the range of 4-3127 km³ (0.5-3769 km³ in *Crown et al. (2003)*), averaging at 299 km³ (310 km³). Total relief of aprons range from ~90 m to over 3000 m. *Crown et al. (2003)* related apron heights to the maximum length of aprons (H/L-values) and compared these values to values describing flow mobilities from literature on terrestrial systems. While the mean value of ~0.2 corresponds to terrestrial pyroclastic flows or dry avalanches, the generally wide range of H/L values (0.01-1.4) covered by LDA measurements would also include other debris-flow systems. A genetic connection based on morphometry alone could therefore not properly be established.

A global morphometric analysis of debris aprons and remnant massifs was also carried out by *van Gasselt et al. (2002, 2003a)*. There, emphasis was put on measurements in Mareotis Fossae/Tempe Terra in order to derive differences in volume and area ratios that might indicate a climatic influence. The area and volume ratios of individual mesas and aprons are considered to represent values that could be compared in later work with other areas on Mars to show regional

differences in the state of degradation.

It was shown in *van Gasselt et al. (2003a)* that there is a distinct trend when relating the remnant's surface area to the much larger surface area of the debris apron which is represented by a factor of ~2.5; a value that compares closely to ratios of rock glacier research in terrestrial systems (see table 3.2). A near-constant factor of 1.1 was obtained when volumes of remnant massifs and apron volumes were compared. It was suggested from these results that if there is a possible connection to climatic control during formation of debris aprons, constant ratios would indicate that an equilibrium had been reached, i.e., aprons and remnants reached a fixed size ratio. Apron surface areas and volumes in Mareotis Fossae/Tempe Terra are considerably smaller when compared to results in Hellas Planitia (*Crown et al., 2002, 2003*) with maximum apron surface areas smaller than 630 km² and volumes being less than 200 km³. More detailed description and results on the methodologic approaches and implications – also in comparison with other work – are presented in part III of this thesis.

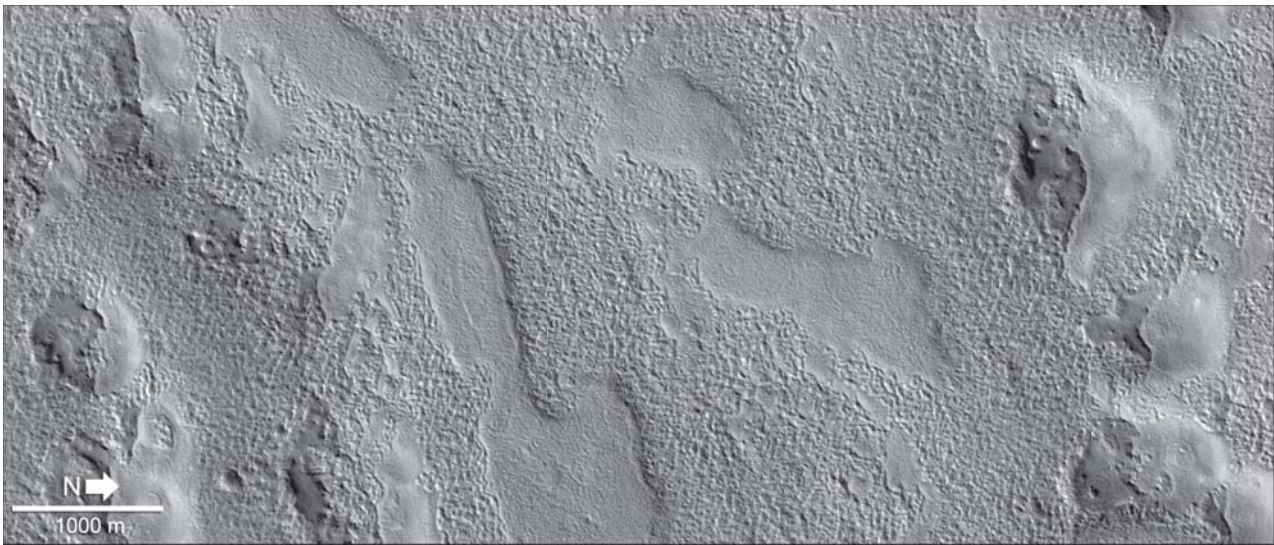


Figure 3.16.: Advance of dissection (pitted surface) in mantled terrain due to sublimation processes, MOC-NA scene FHA01450, location 121°E, 43.5°S, Terra Cimmeria, e' Hellas Planitia, illumination from right, different location of MOC image mentioned in *Mangold et al. (2000d)*.

Nearly 30 years after the discovery of debris aprons as potential rock-glacier analogues, two paper contributions from terrestrial rock-glacier research side have been published in which these landforms are discussed.

Degenhardt and Giardino (2003) discussed the use of ground penetrating radar for the detection of subsurface water in rock glaciers on Mars in order to develop an understanding of processes involved in their formation. A similar approach was also briefly suggested by *Mangold (2001, 2003)*. Although the paper by *Degenhardt and Giardino (2003)* discusses more technical issues and does not provide much detail on Martian landforms, the authors discuss some of the differences between water/ice storage and flow in terrestrial and Martian rock glacier systems (figure 3.13).

Morphological studies were carried out by *Whalley and Azizi (2003)* who performed a short review on terrestrial rock glaciers and associated landforms such as protalus lobes and protalus ramparts and compared these to possible Martian analogs in Candor Chasma, located in the equatorial Valles Marineris system, using MOC wide-angle image data. Results of this study could have severe implications

on the interpretation of rock-glacier landforms on Mars as the possible occurrence of such features in Candor Chasma is far beyond the limits of global debris aprons occurrences as analysed by *Squyres (1979)*. They conclude, however, that an unambiguous interpretation was not possible and that modeling could improve the situation regarding the physical behaviour of ice-rock mixtures. Except for initial work by *Turtle et al. (2003)*, no modeling attempts on the deformation of ice and debris of Martian lobate debris aprons was performed thus far. The Martian landform discussed in *Whalley and Azizi (2003)* need thorough review with new data available from new experiments, as the theoretical implications on Martian climate implied by the findings of *Whalley and Azizi (2003)* would be too large to be ignored if they turn out to be correct (figures 3.14 and 3.15).

3.2.1.4. Debris-Apron Degradation

Mangold et al. (2000c,d) focused on the northern hemispheric LDA and performed a search for landforms on the basis of MOC-NA image data in order to find different units of dissections, i.e., undissected, partially dissected and completely dissected

terrain as manifested by larger abundances of small knobs and buttes the more dissected the terrain becomes. They attribute the dissection patterns to thermokarstic degradation in agreement with patterns identified by *Mustard and Cooper (2000)* that are connected to the 35°-55° northern and southern latitude belts. The distribution is probably controlled by the stability of ground ice in latitudes around 30°-60° as modeled by *Fanale et al. (1986)*. The process responsible for landscape degradation was suggested to be sublimation of ground ice initiated at fractures (*Mangold et al., 2000c,d; Mangold, 2003*) which subsequently led to characteristic pitted and dissected thermokarst landforms (also confirmed by *Carr (2001)*).

For the southern-hemispheric circum-Hellas Planitia and the northern-hemispheric Mareotis Fossae populations of lobate debris aprons attempts were made to correlate and interpret different textural properties of debris aprons. *Pierce and Crown (2001)* and *Crown et al. (2002)* observed sharp ridges indicative of degradation of the uppermost surface layer and concluded that loss of volatiles was responsible for the characteristic pitted surface.

Morphometric comparison work regarding debris apron populations in Mareotis Fossae and Hellas Planitia was conducted by *Chuang and Crown (2005b)* on the basis of earlier work (*Pierce and Crown, 2001; Crown et al., 2002; Chuang and Crown, 2004a,b, 2005a*). They showed that the morphometric key values, such as areas and volumes, are generally smaller in the Mareotis Fossae region than in Hellas Planitia by a factor of ~2-3. These estimates are consistent with values obtained by *van Gasselt et al. (2003a)*. They concluded that smaller height-to-length ratios in Mareotis Fossae speak for larger percentages of volatiles. Work on the morphologic inventory of the Mareotis population resulted in the detection of six surface textures that belong (a) to an upper surface mantle that shows different stages of degradation and (b) to a lower group that is exposed when the upper surface mantle is removed. They concluded that this upper mantle is comparable to the global ice-rich mantle detected also in Deuteronilus Mensae and

which was discussed by *Mustard et al. (2001)* and also *Hauber et al. (2002)* for the Mareotis Fossae region. *Chuang and Crown (2005b)* summarized that the degradational process of the upper layer results in a pitted, ridge-and-valley texture controlled by sublimation comparable to thermokarst processes. They also suggested that the mantle might be comparable to dusty, silty or even sandy material. Comparison of Mareotis Fossae and Hellas Planitia debris aprons with the help of THEMIS IR image data has provided additional support on this view as day- and nighttime temperature variations derived from infrared radiation has shown compositional differences of debris aprons and remnants (see also *Piatek et al. (2004)*). Apron surfaces are slightly colder in nighttime temperatures when compared to adjacent terrains and remnant surfaces. *Chuang and Crown (2005b)* concluded that the mantling in Hellas Planitia has probably vanished already as nighttime temperatures imply high rock abundances in contrast to the implied high abundance of unconsolidated masses in Mareotis Fossae.

3.2.1.5. Age Estimates

Relative age determinations as performed on the basis of crater counts led *Squyres (1978)* to the assumption that the Nilosyrtris Mensae region (68°E) might be older than Protonilus Mensae (49°E) although a debris mantle found in Protonilus might mask the true ages (*Squyres, 1978; Carr, 1995*). The highland terrain nevertheless shows a higher crater density than the northern lowlands and valleys of the fretted terrain, indicating younger ages for lineated valley fill and providing additional support for the ground-ice theory by *Sharp (1973)*. The relatively pristine appearance of debris aprons indicated that flow might have even occurred in more recent times and is therefore considered to be much more recent than degradation of the terrain adjacent to aprons (*Squyres, 1978*). Two mechanisms could account for this, either apron formation is a process different from highland degradation or remnant degradation and apron formation are processes that were reactivated in more recent times

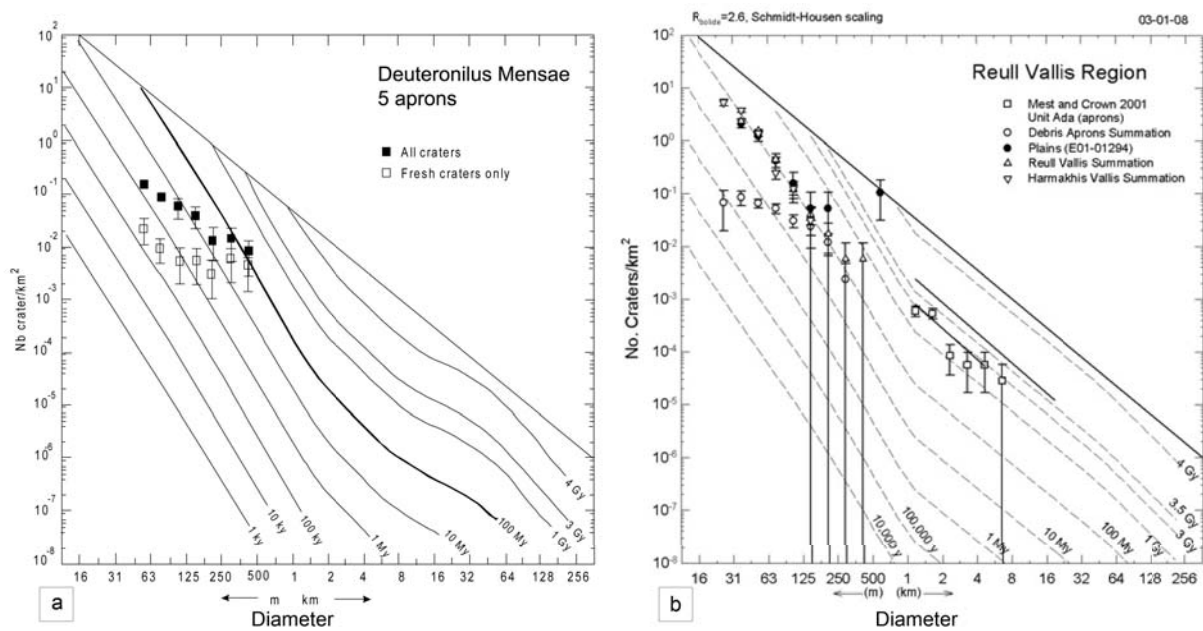


Figure 3.17: Crater-size frequency distribution measurements on debris aprons, [a] five lobate debris aprons in Deuteronilus Mensae and derived ages, from *Mangold (2000)*; [b] measurements on debris apron and Reull Vallis floor in Eastern Hellas Planitia, modified after *Berman et al. (2003)*.

(*Squyres, 1978*).

The interpretation by *Squyres (1978)* is not shared by *Lucchitta (1984)*. Although debris aprons show few craters only, formation of the fretted terrain could have occurred between 0.6 Ga to 3.7 Ga ago and took place over a period of 100-300 Ma. As degradation and apron-formation processes were considered to be essentially the same process, *Lucchitta (1984)* proposed that obliquity cycles on the scales of $1.2\text{-}12 \times 10^5$ a, coupled with cycles of eccentricity ($95\text{-}2000 \times 10^3$ a) and precession cycles (51×10^3 a) as based on the models by *Murray et al. (1973)*; *Pollack (1979)*; *Toon et al. (1980)* and *Ward (1974)* might have caused a movement of regions of ice stability towards the equator. These cycles would have caused intermittent debris apron formation and subsequent removal of debris through desiccation and/or perhaps aeolian processes.

Lucchitta (1984) furthermore concluded that these cycles might have occurred up to 30,000 times since 3 Ga ago and that the missing amount of debris which must have been removed from the fretted terrain, was distributed over wide areas. According to *Lucchitta's*

theory, this would also imply that the debris aprons would consist of much more ice than anticipated before and that they would be more akin to glaciers than to rock glaciers. This way, ice could sublimate and leave behind only few amounts of debris only. Indicators for disintegration and thermokarst-like processes are numerous hollows and pits on debris apron surfaces (figure 3.10). Two years later, the theory on orbital changes was used also by *Squyres and Carr (1986)* to interpret their observations and it was reactivated in recent time again.

Mangold (2000, 2003) investigated crater diameters and crater degradation morphologies of debris apron surfaces in the fretted terrain of the dichotomy area. It was noticed that craters on lobate debris aprons can be categorized according to the degree of relaxation, degradation and deformation. Degraded craters were considered to be generally older than fresh-appearing craters and derived ages of a few million years as obtained using the chronology model of *Hartmann et al. (2000)* indicate either that the last episode of degradation occurred during the last 100 Ma in connection with climate change, or that degradation is sim-

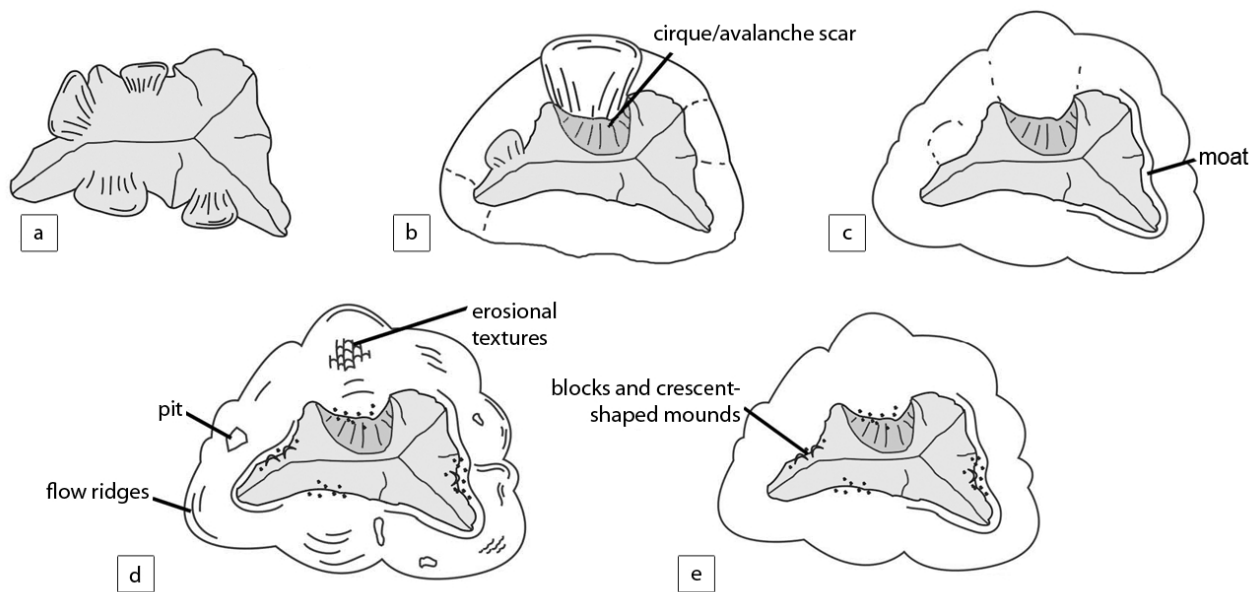


Figure 3.18.: Model for debris apron formation with [a] emplacement, [b] coalescence and continued large-scale emplacement, [c] post-emplacement flow, [d] small-scale mass wasting, [e] wind ablation and thermokarstic degradation, slightly modified after *Pierce and Crown (2003)*.

ply a long-term process. It was suggested that the last active phase was approximately 100 Ma ago and that degradation continued until recently (*Mangold, 2000*). Similar results were obtained by *Berman et al. (2003)* indicating ages around 100 Ma for the southern hemispheric Reull Vallis and much younger ages for debris aprons according to the method of *Hartmann and Neukum (2001)* (figure 3.17). The pronounced flattening of the crater-size frequency curve towards smaller crater diameters as seen in the debris apron measurement indicates multiple episodes of activity (*Berman et al., 2003*). Young ages of < 100 Ma were also confirmed later by *Li et al. (2005)*.

Planimetric values for lobate debris aprons as derived by *Crown et al. (2002)* were used to estimate resurfacing rates in Eastern Hellas Planitia and were compared to resurfacing rates on a global scale (*Crown et al., 2002*). As debris aprons are considered to be of Amazonian age (e.g., *Mest and Crown, 2001*), resurfacing rates are consequently 1×10^{-5} km²/a (for an Hesperian-Amazonian boundary at 3.1 Ga ago), and about 1×10^{-4} km²/a if the Late Amazonian is taken into account which spans the last 300-600 Ma. The

obtained value is 10-100 times lower than common estimates for the Amazonian (*Tanaka et al., 1992*).

3.2.1.6. Source of Debris and Ice

Two hypotheses have been proposed thus far to explain the possible source of debris that was incorporated into debris-apron formation: one theory suggests rock-fall mechanisms (*Squyres, 1978; Colaprete and Jakosky, 1998*), the other one favours landsliding for debris accumulation (*Lucchitta, 1984*). In order to shed light on this debate, *Mangold and Allemand (2001)* related the volume that accumulates under a scarp to the volume of a debris apron by integrating the equation of a parabola (see equation 3.21). Their results have shown that the volume of debris aprons is equal to or larger than the volume of eroded material by rock fall which would indicate that landsliding was the primary process for apron formation. Regarding the source of ice, i.e., atmospheric vs. ground ice, *Mangold et al. (2000a); Mangold and Allemand (2001)* discussed that the incorporation of atmospheric ice is limited to the upper decimeters of debris and that this

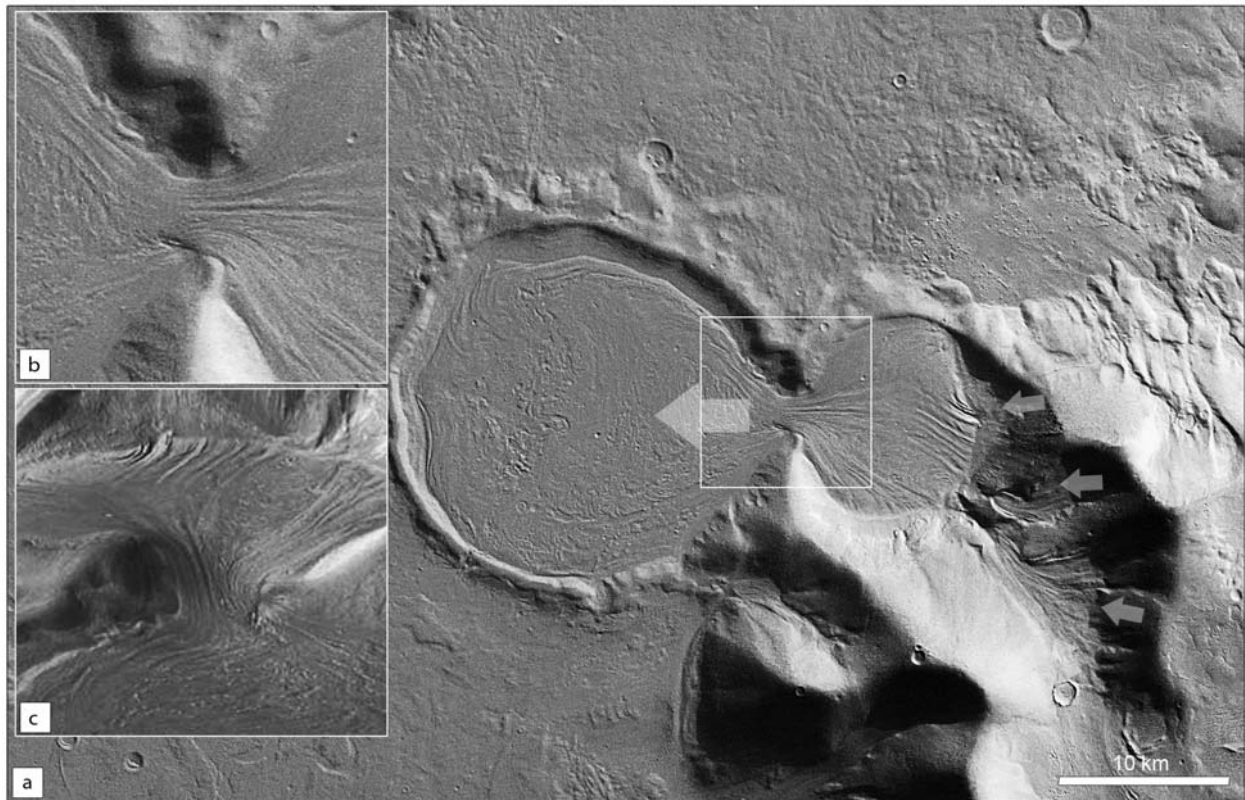


Figure 3.19.: Hour-glass-shaped flow in [a] crater east of the Hellas Planitia impact basin, interpreted as glacial flow (*Head et al., 2005*) and dated to have been active ~ 40 Ma ago. Arrows indicate direction of debris transport. Detail [b] shows confined flow through narrow valley connecting upper and lower impact crater; [c] perspective view; scene from HRSC orbit 451, located at 97.2°E , 43.2°S , see *Head et al. (2005)* for in-depth discussions.

process is unlikely to have significantly contributed when landsliding is considered as the primary mechanism. Instead, ice that was available in plateau material, as also suggested earlier by, e.g., *Lucchitta (1984)*, could be transported downslope together with debris and deform subsequently.

Earlier work by *Mangold et al. (2000b)* has shown that scarps of the fretted terrain might consist of significant amounts of ice as their slopes have angles of 15° – 25° and are much less inclined than the internal friction of rock materials would allow.

Pierce and Crown (2003) reported on the Hellas Planitia debris apron population and suggested catastrophic large-scale mass wasting as well as gradual (peri-)glacial creep processes as responsible for formation of aprons. Blocky material, mounds and ridges suggest furthermore ongoing small-scale mass

wasting after the main emplacement. Degradation pits and an upper sharp-ridged surface indicate furthermore thermokarst-like degradation (see above). The authors also prefer a rock-glacier origin over an origin by debris-covered glaciers as indicators for an icy interior of these flows are missing. Since the current climate is not conducive to apron formation, large deflation landforms would be expected but are however not observed (see also figure 3.18).

3.2.1.7. Examples of Transitional Morphologies

Lobate debris aprons can have different appearances and can be accompanied by landforms that are identical in, e.g., textural properties but which have a completely different shape. Such a special case of debris aprons is seen in the Eastern Hellas Planitia assemblage of lobate debris aprons. There, a spatu-

late landform shows significant morphological differences from adjacent lobate debris aprons. Although its shape is considerably different, it has often been shown in rock-glacier related work on Mars (*Crown et al., 1992; Baratoux et al., 2002; Degenhardt and Giardino, 2003; Pierce and Crown, 2003; Kargel, 2004*). The landform was controversially discussed either as a rock-glacier analog (e.g., *Crown et al., 1992; Degenhardt and Giardino, 2003*) or as a wet debris avalanche by *Baratoux et al. (2002)*. Later work has shown that a landslide origin is probable but that resurfacing and re-mobilization of this landform due to high ice contents and cold-climate modification is very likely (*van Gasselt et al., 2007*). Details on this work and a review of the literature related to this elongated landform are discussed in part III of this thesis.

Another unusual feature is also located in the Eastern Hellas Planitia/Promethei Terra region (figure 3.19), which was interpreted as glacial feature (*Head et al., 2005*) and which forms one of an abundance of other landforms interpreted as indicators of former extensive glaciation (e.g., *Head et al., 2005, 2006b,a; Garvin et al., 2006*). In their work, terrestrial cold-based glacial systems from Antarctica are frequently compared to Martian debris-apron landforms and their evolution is connected to obliquity changes in the Martian spin-axis, similar to the approach first mentioned by *Lucchitta (1984)*. *Head et al. (2005)* found evidence for glaciation for debris-filled craters in eastern Hellas Planitia that were considered to have been active ~40 Ma ago (minimum age). The configuration is interpreted to be similar to the terrestrial Malaspina piedmont glacier with a valley glacier terminating and spreading on the foreland plains. *Head et al. (2005)* also saw multiple episodes for resurfacing on the basis of crater size-frequency data and found supporting morphologic evidence for superposition of rock glacier lobes on Olympus Mons debris-covered piedmont glaciers (see also figure 3.25). Ages of older than 130 Ma for the large lobes confirmed that the Martian spin-axis varies with time and was at higher obliquities during formation of the Olympus Mons glacial lobe. *Head et al. (2006b,a)* summarize that formation of lineated valley fill and debris aprons at the Mar-

tian dichotomy boundary was connected to regional snow and ice accumulation which compared closely to terrestrial intramountain glacial landforms. Further observations for glacial processes have been reported from other locations of the dichotomy boundary or areas in the same latitude range, such as the Acheron Fossae (*Dickson et al., 2006a*), Nilosyrtis Mensae (*Levy and Head, 2006a,b*) or the Arabia Terra area in general (*Nahm et al., 2006; Dickson et al., 2006b; Head and Marchant, 2006; Kress et al., 2006*).

3.2.1.8. Deformation and Rheology

Discussions on the deformation and rheology of lobate debris aprons are almost exclusively connected to the cross-section profile of these features and the theoretical considerations by *Paterson (2001)* for terrestrial glacial ice sheets. For this reason, the background and derivation of the theoretical profile is summarized in the box "The Cross-Section Profile of Ice Sheets" on page 53. First work discussing this approach for the Martian case was published by *Squyres (1978)*. Squyres' considerations on deformational processes have been revived three decades later with more precise data and are frequently applied today. In support of terrestrial work on rock glaciers, *Squyres (1978)* summarizes that rock glacier behavior is comparable to high viscosity fluids with apparent viscosities ranging from $2\text{-}9\cdot 10^{14}$ Pa·s to $50\text{-}90\cdot 10^{14}$ Pa·s according to *Wahrhaftig and Cox (1959)* and *White (1971)*, respectively, and which have a basal shear stress of around 100 kPa similar to polycrystalline ice with a plastic behavior and a yield stress of 100 kPa. The deformation law as described by *Glen (1952)* and *Glen (1953)* is still considered to be valid and has also been used for Martian rock glacier analogues:

$$\dot{\epsilon} = A\tau^n, \quad (3.4)$$

with $\dot{\epsilon}$ [a^{-1}] being the strain rate, τ [Pa] being the stress and A and n being constants with $n \sim 3.5$. The factor A is temperature dependent (see also section 3.1.4.1 on terrestrial rock glaciers). As the basal shear

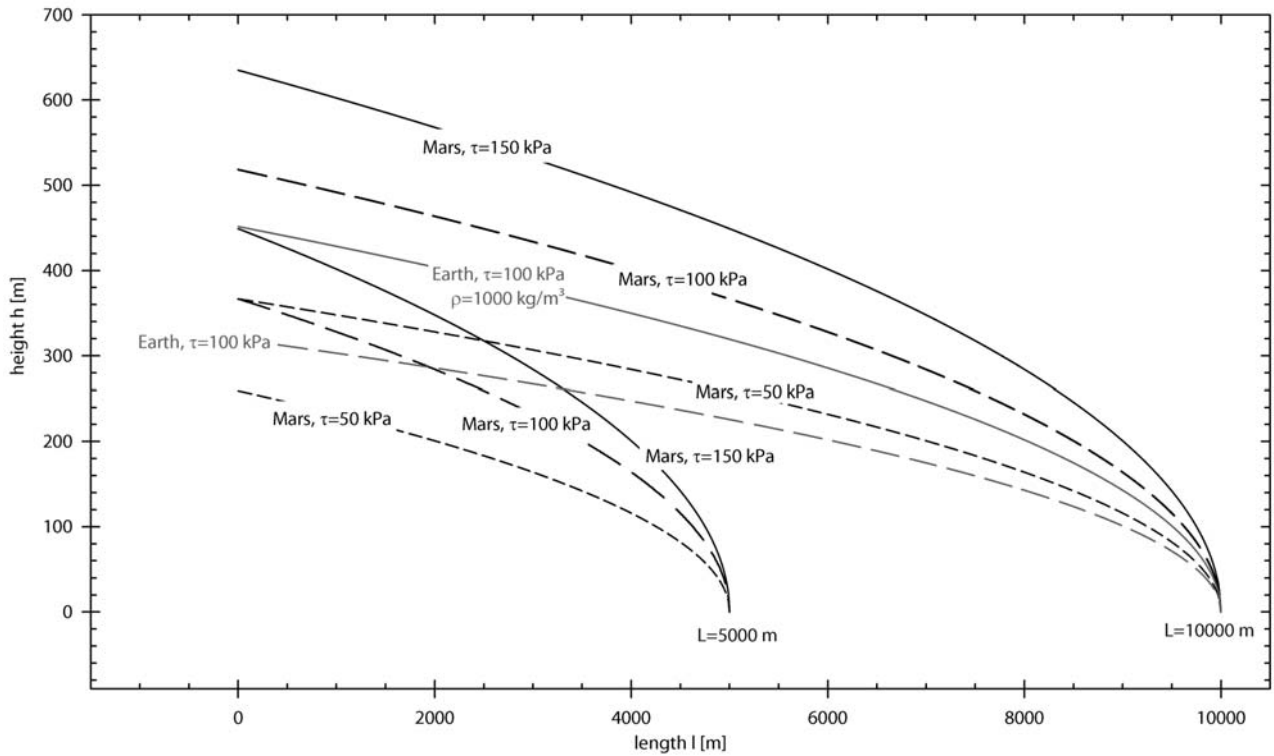


Figure 3.20.: Theoretic profiles of debris aprons and symbols used for derivation of flow rheology (*Paterson, 2001*). Shapes are representations of equation [4] and [5] in *Paterson (2001)*, p. 242 assuming a basal shear stress τ of 50, 100, and 150 kPa and a length L of 5000 m and 10000 m. Note variations in total heights for terrestrial and Martian cases Black parabolas represent Martian cases with acceleration due to gravity of $g = 3.72 \text{ m/s}^2$; gray parabolas represent terrestrial cases with acceleration due to gravity of $g = 9.81 \text{ m/s}^2$. Material density is $\rho = 2000 \text{ kg/m}^3$ for ice-debris mixtures. For comparison see parabola with $\rho = 1000 \text{ kg/m}^3$ for pure water ice.

stress does not exceed the yield stress, viscous deformation does not occur under present climatic conditions (*Squyres, 1978*)

$$\tau_b = -\rho gh(dh/dx), \quad (3.5)$$

with τ_b [Pa] being the basal shear stress, ρ [$\text{kg}\cdot\text{m}^{-3}$] being the material's density, g [$\text{m}\cdot\text{s}^{-2}$] is the gravitational acceleration, h [m] is the material's thickness, and x [m] is the length of the debris apron measured from the escarpment. The shear rate $\dot{\gamma}$ can be calculated using

$$\dot{\gamma} = \tau/\eta = -\rho gh(dh/dx)/\eta, \quad (3.6)$$

where η [Pa·s] is the viscosity.

Advance is then calculated over the whole length as

follows

$$-\int_0^L [-\rho gh(dh/dx)/\eta] dx = \rho gH^2/2\eta, \quad (3.7)$$

with L [m] being the overall length of the debris apron and H [m] being its overall thickness (see figure 3.20). *Squyres (1978)* assumed values for the unknown thickness H and a material density of $\rho = 2000 \text{ kg/m}^3$ and obtained advance values of 60 m/a, that are, however, far too high. *Squyres* could not think of any process providing the amount of material to obtain viscous flow even if viscosity estimates would have been completely wrong. He concluded finally, that the debris is in equilibrium, i.e., basal shear stress is equal to the yield stress. *Squyres (1978)* also mentioned that the yield stress τ_o of any debris apron can be approximated using the relation by *Orowan (1949)* (as cited

in *Squyres (1978)*) in the way

$$\tau_o = \rho g H^2 / 2L \quad (3.8)$$

and that the approximate values for debris aprons using shadow measurements fall fairly well into the range of a 100 kPa yield stress as given by *Wahrhaftig and Cox (1959)* for terrestrial systems. *Squyres (1978)* concludes his flow-model summaries by referring to the general parabola equation (*Paterson, 2001*) that describes the theoretic shape of such an apron (see also derivation of equation 3.21).

Squyres (1978) states that at least 30% of ice must be included in the debris to facilitate creep of material. In general lack of topographic data prior to MOLA-aided research in the late 1990s, stereo-models of Viking data have provided some insights into the topography. *Ewing and Schenk (1998)* derived stereo-models and used obtained values for sample locations in Protonilus Mensae and Hellas Planitia and determined that scarp heights are in the range of up to 5 km and apron thicknesses are between 300 m to 1000 m. In contrast to *Squyres (1978)*, *Ewing and Schenk (1998)* assumed the average density of material to be around 1800 kg/m³ and calculated the linear factor *A* for strain rates according to Glen's law through the Arrhenius equation

$$A = A_o \cdot e^{-Q/RT}, \quad (3.9)$$

with *A_o* being 4.3 × 10⁻⁴ s⁻¹ kPa⁻³, *Q* = 60 kJ mol⁻¹ for *T* < 263 K being the activation energy and *R* is the gas constant. Flow velocities were estimated according to *Paterson (1994)* (see equation 3.21). They concluded that at least 50% of ice is needed to facilitate flow at a rate of 5 mm/year with $\tau_b = 210$ kPa, and an average thickness of 550 m. The thickness values are larger than estimates by *Zimbleman et al. (1989)* who concluded that strain rates are far too low for ice to creep under current climatic conditions.

Lucchitta (1984) reviews processes proposed by *Squyres (1978, 1979)* and concludes that at lower latitudes ice may flow when values for debris apron thicknesses of 500-800 m and average densities of 2000 kg/m³ (*Squyres, 1978*) are assumed; basal shear

stress is considered to be between 1.4-4.6 × 10⁴ Pa. According to the ice-deformation map of *Shoji and Higashi (1978)*, ice at temperatures above 150 K fall into the field of dislocation creep which translates to the dominant deformation mechanism for terrestrial glaciers. At lower temperatures, i.e., polewards, ice is deformed by boundary-diffusion creep and ice may not flow anymore. Further analyses carried out by *Lucchitta (1984)* in filled channels of the fretted terrain suggest that the basal shear stress τ_b required for flow of terrestrial glaciers and rock glaciers must exceed at least 10⁵ Pa. Considering maximum debris thickness of less than 1 km and slopes of 5-8 m/1000 m the resulting stresses would be 1.2-2.6 × 10⁴ Pa for ice with $\rho = 900$ kg/m³, 2.7-5.7 × 10⁴ Pa for rock glaciers with $\rho = 2.0$, and 3.4-7.1 × 10⁴ Pa for rock with $\rho = 2.5$ kg/m³. None of these stresses exceed the 10⁵ Pa limit (*Lucchitta, 1984*). *Lucchitta* considers dislocation creep mechanisms for flow at very low strain rates of 10⁻¹³ s⁻¹ and compares that with gravitational spread of rocks on the Earth. Other explanations target on unfrozen brines or even clathrates instead of ice.

First thorough analytical work was carried out by *Colaprete and Jakosky (1998)* discussing the possibility of ice flow and formation of rock glaciers on Mars. Their modeling results have the following implications: (1) under present mid-latitude temperatures of about 210 K, ice and debris cannot move, i.e., the mixture becomes too rigid to deform and would require temperatures 20-40 K higher than today, (2) ice content must be at least 80% to facilitate flow, and (3) net accumulation rates must be on the order of 1 cm/a to provide the debris input required for flow. Slightly different results were suggested by *Mangold et al. (1999)* on the basis of experiments on the deformation of ice. Assuming mean temperatures at typical locations for lobate debris aprons of 215-220 K, stresses (i.e., basal shear stress) of about 10⁵ Pa, and average apron sizes of *L* = 10 km, timespan for apron formation would be on the order of 100 Ma to 1 Ga and a factor of 10% less if temperatures were 20 K higher. The authors derived strain rates of 10⁻¹⁵ s⁻¹ but considered these results questionable. However, *Mangold et al. (1999)*

EXCURSION: THE CROSS-SECTION PROFILE OF ICE SHEETS

The background for the theoretic parabola shape of a cross section cutting through a debris apron is based upon a model explained by *Paterson (1994)* (based on *Paterson (1981)*) for terrestrial glacial ice sheets. This model was utilized frequently afterwards by various workers in order to demonstrate that Martian debris aprons were indeed rheologically comparable to glacial landforms and that therefore the prominent constituent in debris aprons had to be ice. Two derivations lead to a function describing the parabolic shape of an ice sheet assuming perfect plasticity; first by using the shear stress relationship, secondly by using mean velocities under assumption of laminar flow.

For the shear-stress relationship, the driving stress τ of a slab of ice on an inclined plane whose surface is parallel to its base is balanced by the basal drag, i.e., the shear stress at the base τ_b

$$\tau_b = \rho g h \cdot \sin \alpha \longrightarrow \tau_b = -\rho g h \frac{dh}{dx}. \quad (3.10)$$

Measurements have shown that τ_b is between 50 kPa and 150 kPa and therefore ice is considered as a perfect plastic material with a yield stress of $\tau_o = 100$ kPa. For small angles between the base and the surface slope of the ice slab this relation has shown to be valid also (see *Paterson, 1994*, p. 241 for derivation). In the case of perfect plasticity, ice thickness adjusts so that $\tau_b = \tau_o$ at every point and integration of equation 3.10 gives

$$h^2 = \frac{2\tau_o}{\rho g} (L - x). \quad (\text{see figure 3.20}) \quad (3.11)$$

A second approach for obtaining a theoretic cross profile is by using the flow relation for ice according to *Vialov (1958)* as cited in *Paterson (2001)* by making use of the average velocity u . If laminar flow is assumed, i.e., stress occurs in the τ_{xz} plane, and velocities in z-direction are zero, it follows from the stress-strain relationship $\dot{\epsilon}_{xz} = A\tau_{xz}^n$ by *Glen (1952)*

$$\dot{\epsilon}_{xz} = \frac{1}{2} \frac{du}{dz} \quad (3.12)$$

$$A\tau_{xz}^n = \frac{1}{2} \frac{du}{dz} \quad (3.13)$$

According to equation 3.10:

$$\tau_{xz} = \rho g (h - z) \sin \alpha. \quad (3.14)$$

Integration then gives velocities

$$u_s - u(z) = \frac{2A}{n+1} (\rho g \sin \alpha)^n (h - z)^{n+1} \quad (3.15)$$

$$u_s - u_b = \frac{2A}{n+1} (\rho g \sin \alpha)^n h^{n+1}. \quad (3.16)$$

Further integration yields mean velocities

$$\bar{u} - u_b = \frac{2A}{n+2} (\rho g \sin \alpha)^n h^{n+1} \quad (3.17)$$

$$\bar{u} = \frac{2A}{n+2} \tau_b^n h. \quad (3.18)$$

Assuming steady state and an accumulation of ice with a thickness c and ablation it follows

$$cx = h\bar{u} = \frac{2A}{n+2} \left[-\rho g h \left(\frac{dh}{dx} \right) \right]^n \cdot h^2 \quad (3.19)$$

The solution to this equation is

$$h^{2+2/n} = \left[\frac{2(n+2)^{1/n}}{\rho g} \cdot \left(\frac{c}{2A} \right)^{1/n} \right] \cdot (L^{1+1/n} - x^{1+1/n}). \quad (3.20)$$

Here, $h = H$ for $x = 0$

$$(h/H)^{2+2/n} + (x/L)^{1+1/n} = 1 \quad \text{with } n \rightarrow \infty \text{ for perfect plasticity.} \quad (3.21)$$

For detailed reference and in-depth discussion the reader is referred to *Paterson (2001)*, p. 241ff.

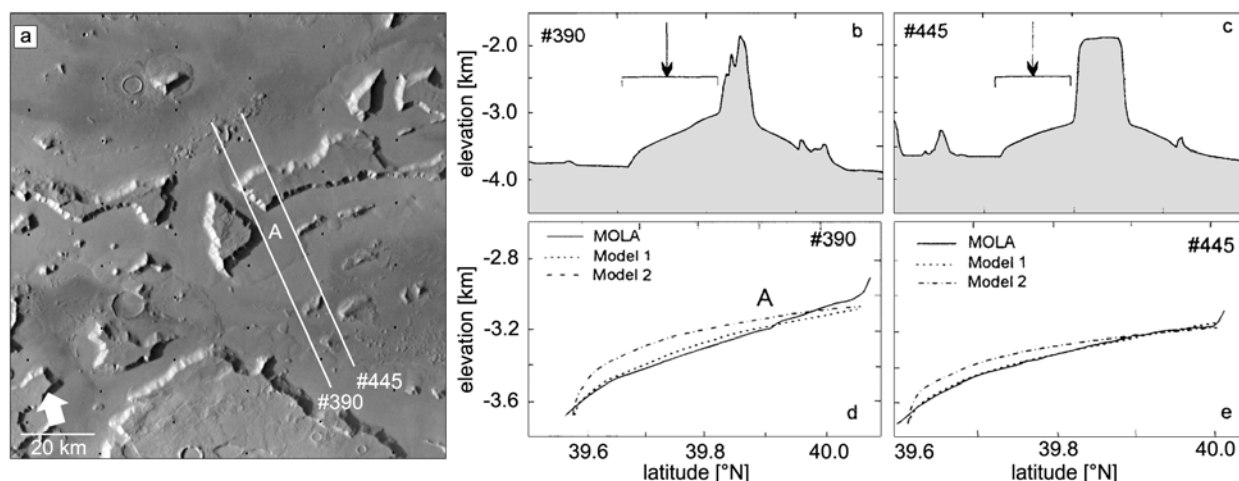


Figure 3.21.: Lobate debris aprons in Deuteronilus Mensae and topographic profiles as obtained by *Mangold and Allemand* (2001), model 1 refers to theoretic profiles as derived for plastic equilibrium, model 2 refers to viscous power law, modified and adjusted after *Mangold and Allemand* (2001).

assumed that an ice content of 30% would be required to maintain activity of rock glaciers on Mars.

In the post-Viking era, only few modeling attempts have been made and the theoretical approaches performed during that time have more or less confirmed what has been approximated in earlier work by, e.g., *Squyres* (1978, 1979). *Mangold and Allemand* (2001) revived some of the theories put forward by *Squyres* (1978) with respect to theoretical profiles that can be fit to the cross-section shape of debris aprons. While that work was initially performed on photoclinometrically derived values, *Mangold and Allemand* (2001) made use of newly available MOLA topographic data. Assuming a flat base, *Mangold and Allemand* (2001) derived values for the basal shear stress according to equation 3.5 with the assumption that basal shear stress is equal to the yield stress and has therefore the same value at every location. Parameter n in equation 3.21 represents the power-law exponent and is usually between 1 and 3. When n approaches ∞ , equation 3.21 approaches equation 3.11.

Using measurements of apron lengths (L) in the range of 11-33 km and heights (H) of 275-620 m, *Mangold and Allemand* (2001) obtained theoretical profiles on which topographic MOLA-based profiles have been superimposed (figure 3.21). Although both models fit

in principle to the topographic measurements, theoretical models for plastic equilibrium show a generally better fit leading *Mangold and Allemand* (2001) to the conclusion that debris aprons are indeed controlled by the deformation of debris and ice and that the theory put forward by *Squyres* (1978) is confirmed.

The "perfect parabolic shape" (*Mangold and Allemand*, 2001) of the fit led to the conclusion that no other process except for solid-state creep such as basal sliding would be needed for deformation. As, according to *Paterson* (1994), terrestrial ice sheets fit better to the viscous power law model, *Mangold and Allemand* (2001) deduced that today, debris aprons on Mars are at a plastic equilibrium showing no deformation anymore. For aprons that fit better to the viscous power law model, *Mangold and Allemand* (2001) assumed a state that has not reached equilibrium yet.

Values for basal shear stresses obtained by *Mangold and Allemand* (2001) are in the range of $0.34-1.08 \cdot 10^5$ Pa and are slightly lower than those proposed by *Squyres* (1978) with $0.60-1.30 \cdot 10^5$ Pa. However, they compare closely to shear stresses of terrestrial glacial systems with 0.50-1.50 bar (*Paterson*, 2001) and are slightly lower than those for rock-glacier systems with a yield stress in the range of $1.0-3.0 \cdot 10^5$ Pa (*Whalley*, 1992). *Mangold and Allemand* (2001) explained low

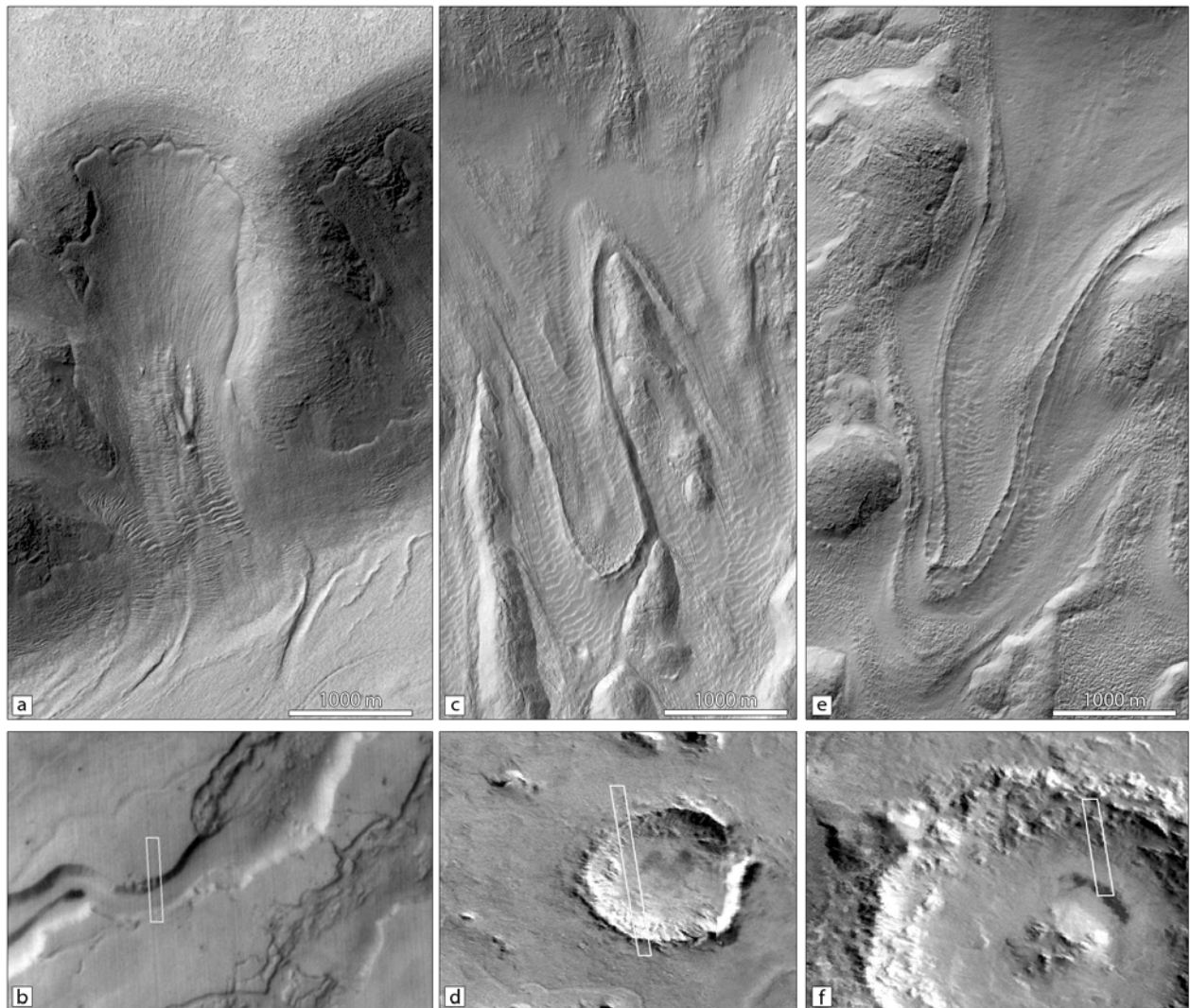


Figure 3.22.: Examples of viscous flow features as selected by *Milliken et al. (2003)*, see text for explanations, [a] MOC-NA Mo3/04950 and [b] context scene, 90.9°E , 35.7°S ; viscous flow features contribute debris to a broad valley that is filled with material comparable to lineated valley fill; [c-f] viscous flow features at south-facing crater-rim: [c] MOC-NA Mo4/02881 and [d] context scene, 111.6°E , 36.0°S ; [e] MOC-NA M18/00897 and [f] context scene, 112.9°E , 38.6°S ; illumination in MOC-NA scenes from the left, scene [d] is illuminated from the top right, scene [f] is illuminated from the right.

yield stresses by low strain rates that occur at the low temperatures common on Mars.

Similar approximations and assumptions were made later by *Li et al. (2004, 2005)* with data from mid-latitude debris aprons in Mareotis Fossae, Deuteronilus- and Protonilus Mensae. Earlier results could be confirmed and *Li et al. (2005)* also suggested that an ice content of 40% would be required to form such debris-apron landforms.

3.2.2. Viscous Flow Features

Viscous flow features are landforms that are similar to lobate debris aprons and associated landforms as they are related to the creep of material at hillslopes. In contrast to debris aprons there is clear observational evidence that these features are formed through movement of a surficial debris layer only. It is, however, still discussed in how far these features are related to glacial ice or whether they are formed by the

creep of a surface debris mantle on Mars.

Viscous flow features merit a separate section in the discussion on creep-related landforms as (a) their tongue-shaped morphology is different from that of debris-apron features and (b) their sizes are far smaller which makes them observable in high-resolution MOC-NA imagery only.

Detailed investigations of viscous flow features were performed by *Milliken et al. (2003)* and their global mapping approach has shown that these features occur mainly within the 30°-60° latitude belts of both hemispheres. Their distribution is comparable to that of lobate debris aprons and similar landforms with a high density of occurrences at 40° and also comparable to the distribution of young water-related gully-activity (*Reiss, 2005; Balme et al., 2006*). More importantly, their distribution is similar to that of a mid-latitude mantling deposit (*Mustard et al., 2001*) that has also been noticed by *Malin and Edgett (2001); Carr (2001); Cabrol and Grin (2002)* on MOC-image scale. That mantling deposit has a thickness of approximately 10 m (*Mustard et al., 2001*) and is distributed in an area where a relatively smooth surface topography and texture has been observed on the basis of MOLA topography data by *Kreslavsky and Head (2000)* and by earlier workers (*Soderblom et al., 1973; Grant and Schultz, 1990; Grizzaffi and Schultz, 1989; Schultz and Lutz, 1988*). Further results of *Milliken et al. (2003)* suggest that viscous flow features are formed within an ice-dust layer of ~10 m thickness which is currently subject to degradation. Ages of these viscous flow features are estimated to be in the range of 0.1-10 Ma (upper limit of 30 Ma) resulting in strain rates on the order of 10^{-16} - 10^{-11} s⁻¹. *Milliken et al. (2003)* conclude that these ice-rich features are genetically related to the global mantling deposit.

The shape and appearance of viscous flow features vary (figure 3.22) but characteristics, such as their lobate form, flow ridges, extensional furrows and compression ridges, surface lineations and the presence of an older degraded material is common to all of them (*Milliken et al., 2003*). Viscous flow features are considered to be older than gullies which dissect those features. It is, however, believed that both landforms

are genetically related to each other, i.e., viscous flow features might have contributed to the formation of gullies through considerable release of water.

Later, *Arfstrom and Hartmann (2005)* reinvestigated these landforms. They considered the same features discussed by *Milliken et al. (2003)* as possible glacier flows (*glacier-like features, GLF*) and compared terminal ridges to glacial moraines and protalus ramparts (*Arfstrom, 2003*). They determined ages using upper-limit estimates and activity phases and found some correlation to obliquity changes around 4-5 Ma ago, contemporary with the formation of the Martian mantling deposit and gullies. In analogy to features observed in the Antarctic Dry Valleys, *Marchant et al. (2003)* developed a descriptive nomenclature for similar landforms, called tongue-shaped lobes, and concluded on the basis of comparison to (a) Antarctic Dry Valley gelifluction lobes, (b) rock glaciers and (c) alpine glaciers that they resemble closely alpine glaciers and debris covered glacier deposits. Processes such as sublimation and melting might have led to retreat of these features leaving behind marginal ridges (*Marchant et al., 2003*). This conclusion was additionally confirmed by the missing convexity of the topographic profile that is considered indicative of inactive creep landforms. Further support for the late-Amazonian icy debris slopes were provided through numerical analyses conducted by *Perron et al. (2003)*.

3.2.3. Fan-Shaped Deposits

Apart from the wealth of landforms indicative of ice-assisted debris movement located at the Martian dichotomy boundary and adjacent areas of the fretted terrain, extensive morphologic analysis work has been conducted on the nature of glacial and/or periglacial landforms located at the Tharsis Montes volcanic constructs in Martian equatorial latitudes and termed fan-shaped deposits (e.g., *Head and Marchant, 2003; Head and Marchant, 2003; Shean and Head, 2003a; Milkovich and Head, 2003*). That work is mainly based upon observations and mapping work made by *Zimbelman and Edgett (1991, 1992)*.

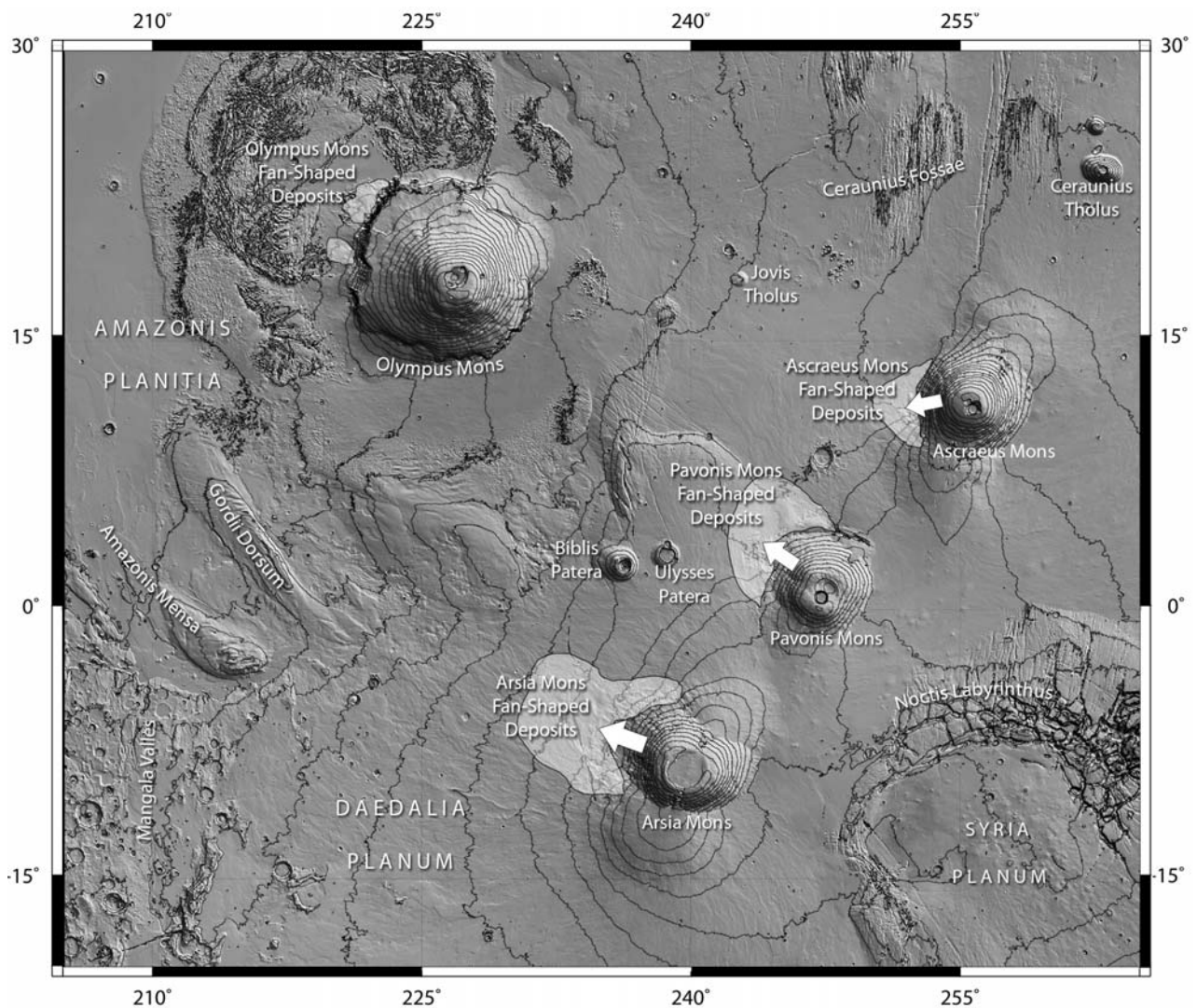


Figure 3.23.: Tharsis volcanic rise with outlines of occurrences of so-called fan-shaped deposits (arrows) indicative of cold-based glaciation at mid-latitudes on Mars (*Head and Marchant, 2003; Head and Marchant, 2003; Shean and Head, 2003a; Milkovich and Head, 2003*); MOLA MEGDR shaded relief map combined with MOC-WA geodesy mosaic for textural details, isolines have a spacing of 1000 m.

Initially, these fan-shaped deposits were interpreted as landslides (*Carr and Schaber, 1977*), pyroclastic flows (*Scott et al., 1998*), glacial landforms (*Scott et al., 1998; Lucchitta, 1981; Zimbelman and Edgett, 1991*), or volcano-glacial features (*Scott et al., 1998*). *Head and Marchant (2003)* have shown that the facies distribution at the western part of Arsia Mons (figures 3.23, 3.24a) is consistent with that of glacial deposits in terrestrial cold-arid regions of Antarctica. The Arsia Mons fan-shaped deposits are up to 450 km wide and extend up to 500 km towards the west. The sur-

face textures as mapped initially by *Zimbelman and Edgett (1991, 1992)* consists of [a] an *outer ridge facies* with arcuate and parallel ridges interpreted as drop moraines indicative of glacier retreat. Towards the center of these ridges, a [b] *knobby facies* is interpreted as sublimation till. Another arcuate ridge facies [c] with convex-outward lobes are interpreted as rock glaciers, some of which are possibly underlain by a core of glacial ice (*Head and Marchant, 2003*). As no meltwater-related landforms are observed, *Head and Marchant (2003)* concluded that these landforms

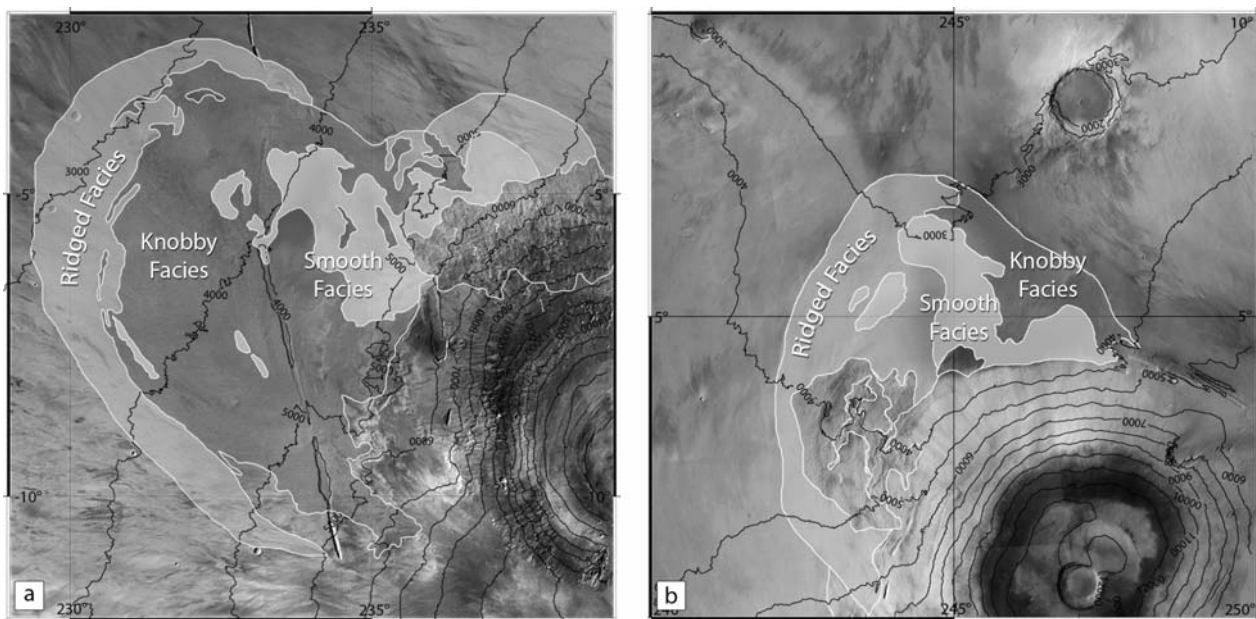


Figure 3.24.: Arsia Mons [a] and Pavonis Mons [b] fan-shaped deposits, after *Zimbelman and Edgett (1991)*; *Head and Marchant (2003)*; *Shean and Head (2003c)*, re-mapped and simplified by author.

are indicative of cold-based glaciation. *Shean et al. (2005c,b)* extended this work by differentiating multiple emplacement episodes at Arsia Mons that indicate not only cold-based glacial activity but also periods of deglaciation connected to the retreat of glaciers. These phases were supported by crater-size frequency measurements and age determinations that yield an age of about 50 Ma to 650 Ma ago (*Shean et al., 2006*). Reconstruction of ice sheets resulted in estimates of 1.6-2.4 km thicknesses for the Tharsis volcanoes and ages for formation of 10-200 Ma ago (*Shean et al., 2004, 2005a*). A prominent elongated basin at the western rim of Arsia Mons that has been filled and overflowed by debris was interpreted as analog area to lineated valley fill areas in the fretted terrain suggestive of similar processes of glaciation also at the Martian highland-lowland dichotomy boundary (*Shean et al., 2005b*) (figure 3.26).

This initial work was extended to similar comparison work at Pavonis Mons (*Shean and Head, 2003a,b,c*) and small areas at western Olympus Mons (*Milkovich and Head, 2003*) with the help of new imagery and topography data. The fan-shaped deposits west of Pavonis Mons (figures 3.23, 3.24b) are half the size of

the Arsia Mons deposits; the textural properties are, however, comparable to those of the Arsia Mons fan-shaped deposits. Moreover, *Shean and Head (2003c)* saw evidence on the basis of MOC-NA and daytime THEMIS-IR image data that the smooth deposits are underlain by residual ice, now covered by debris.

Shean and Head (2003c) furthermore argue that glaciation was probably caused by obliquity changes in Mars' history causing loss and redeposition of polar volatiles in cold traps near the equator. For the large Tharsis volcanoes precipitation might have happened when moisture-rich air masses were forced to move up due to the topographic influence and started to release moisture at the lee side of the volcanoes. This theory was supported by MOC-WA image data showing clouds above the western parts of the volcanoes (see *Shean and Head, 2003c*) and modeling results by *Forget et al. (2006)*. A significant amount of volcanic ash could have contributed and mixed with the precipitated volatiles allowing to form en- and supraglacial debris (*Shean and Head, 2003c*). For Ascraeus Mons, *Parsons and Head (2004)* saw evidence for at least two events of glacial recession and deposition but they do not observe a smooth facies that was

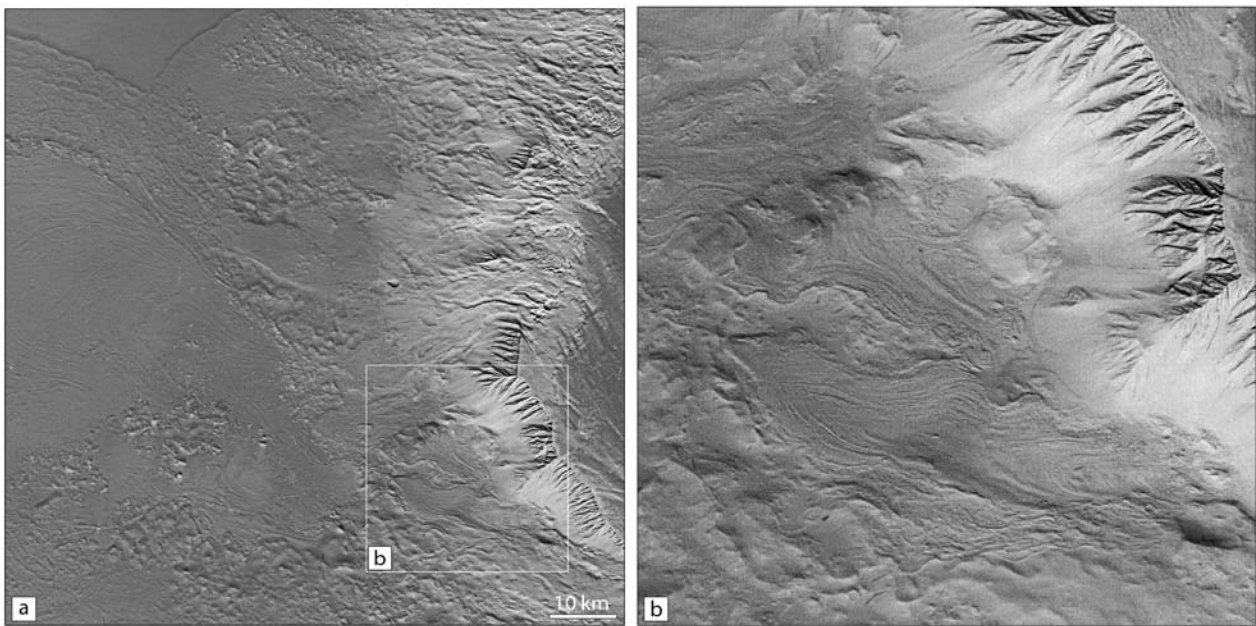


Figure 3.25.: Creep-related landforms at the western scarp of Olympus Mons, [a] arcuate moraine-like ridges described by, e.g., *Lucchitta (1981)*; *Head and Marchant (2003)*; *Head et al. (2005)* and several elongated flow features described as possible rock-glacier analogues, see [b] for more detail, HRSC nadir scene from orbit 0143 (09), scene centered at 221.0°E 19.7°N . North is up, illumination is from the lower left.

found at the Arsia and Pavonis Montes confirming the results of *Zimbelman and Edgett (1991)*. Reasons for this difference were not known but there might be some connection to a special topographic situation or the volcanic evolution of Asraeus Mons (*Parsons and Head, 2005*).

For Olympus Mons, possible glaciation was already suggested early by *Lucchitta (1981)* on the basis of Viking image data. This view was later confirmed by comparative analysis work by *Milkovich and Head (2003)* in the course of their studies on the fan-shaped deposits of the Tharsis Montes (figure 3.25). *Milkovich and Head (2003)* observed that the extent of the Olympus Mons fan-shaped deposits is much smaller than for the other Tharsis volcanoes indicating less favourable conditions for glacier formation and perhaps caused by a long-lasting volcanic activity and a higher geothermal flux. Long-lasting volcanic activity was later confirmed by age determinations by *Neukum et al. (2004)* and observations by *Basilevsky et al. (2005, 2006)* on the basis of HRSC data. Other reasons for the small size of the fan-shaped deposits

at Olympus Mons could be the well-pronounced basal escarpment which might have provided a much larger volume of debris when compared to the smaller Tharsis Montes volcanoes (*Milkovich and Head, 2003*). Nonetheless, *Milkovich et al. (2006)* could identify the same facies as for the Tharsis Montes and found observational evidence for multiple episodes of glacial advance and retreat that interacted with volcanic extrusions at Olympus Mons.

3.2.4. Summarizing Comments

At two latitude belts on Mars, on at 40°N , the other one at 45°S and each $\sim 25^{\circ}$ wide, landforms indicative of creep of debris and ice were recognized that are spatially connected to the northern hemispheric fretted terrain and the southern-hemispheric impact-crater basins. These landforms comprise so-called lobate debris aprons associated with the dichotomy escarpment, isolated remnants and mesas, lineated valley fill related to broad valleys incised into the highland terrain, and the concentric crater fill associated with crater infill and characterized by rim-parallel

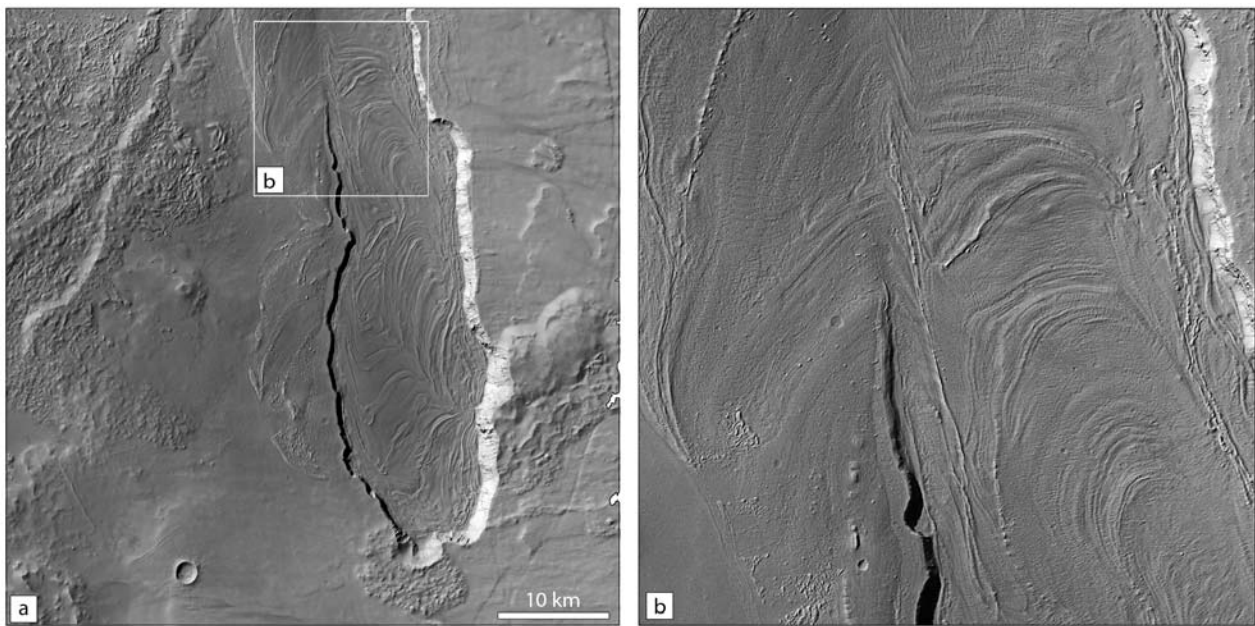


Figure 3.26.: Debris-filled elongated trough at western Arsia Mons [a], initially described by *Lucchitta (1981)*; several debris lobes and an overflowed western rim (see [b]) indicate high-energetic phases of emplacement. Alternative interpretations point towards retreat of former glaciers (*Shean et al., 2005b*), HRSC nadir scene from orbit 1034, scene centered at $236.2^{\circ}\text{E } 7.3^{\circ}\text{S}$. North is up, illumination is from the lower left.

ridges indicating flow of material towards the center of the impact crater.

Debris aprons and associated landforms are considered to be rock-glacier analogs since early Viking-based observations by *Squyres (1978, 1979)*. This conclusion is supported by observations of a convex-upward topographic profile and characteristic surface lineations and a ridge-and-furrow pattern indicating ice-assisted debris creep. The source of debris supply is considered to be either landsliding or rock fall mechanisms. It is still debated in how far disintegration of the Martian highland terrain (fretted terrain) and formation of debris aprons are caused by the same process.

There is a general consensus that debris aprons and associated landforms are geologically young as indicated by the lack of impact craters on medium-resolution image data and just few impact structures visible in high-resolution data. Their age is probably not much older than ~ 100 Ma but intense degra-

dation in more recent time led to disintegration of landscapes probably by sublimation processes and thermokarst. In pre-MGS times a connection between cyclic obliquity changes of Mars' spin axis and precession was established with connection to possible cyclic formation and removal of debris aprons (*Lucchitta, 1984*) and until today it is commonly assumed that formation of debris aprons, lineated valley fill and concentric crater fill are controlled by changes in the orbital parameters of Mars.

Rheologic comparisons with ice sheet models from terrestrial systems gave further support that these landforms are related to the deformation of ice-rich materials. Modelling efforts have shown that current Martian temperatures are not conducive to allow active deformation of ice-rich debris. Volatiles might have been contributed either atmospherically or from the subsurface; recent work, however, has established a connection to the glacial regime where precipitation in Martian history might have been dominant. \square